SUBSPACE BASED ESTIMATION OF THE SIGNAL TO INTERFERENCE RATIO FOR CDMA CELLULAR SYSTEMS

BY DEEPA RAMAKRISHNA

A thesis submitted to the

Graduate School—New Brunswick

Rutgers, The State University of New Jersey

in partial fulfillment of the requirements

for the degree of

Master of Science

Graduate Program in Electrical and Computer Engineering

Written under the co-direction of

Professors Roy D. Yates and Narayan B. Mandayam

and approved by

New Brunswick, New Jersey

October, 1997

ABSTRACT OF THE THESIS

Subspace Based Estimation of the Signal to Interference Ratio for CDMA Cellular Systems

by Deepa Ramakrishna

Thesis Directors: Professors Roy D. Yates and Narayan B. Mandayam

The Signal-to-Interference ratio (SIR) has been highlighted in the literature to be an efficient criterion for several radio resource management algorithms such as power control and handoff. In this paper we address the problem on how to obtain fast and accurate measurements of this quantity in a practical context. We develop a general SIR estimation technique for CDMA cellular systems, that is based on a signal subspace approach using the sample covariance matrix of the received signal.

Analysis and simulation results for an IS-95 like system show that the SIR can be estimated to within 80 percent of the actual SIR after less than 7 frames, or within 90 percent of the actual SIR after less than 15 frames. We also study a computationally less expensive SIR tracking algorithm based on updating the signal subspace. We show that the algorithm works quite well in the context of a rapidly time varying channel.

Acknowledgements

I would like to thank Dr. Roy D. Yates for his patience, encouragement and invaluable suggestions during the work on this thesis. I would like to thank Dr. Narayan Mandayam for getting me started on this project and for his relentless enthusiasm and encouragement throughout the course of this work.

I would like to thank Dr. S. J. Orfanidis and Dr. Jack M. Holtzman for being on my thesis committee.

Finally, thanks are due to the entire WINLAB crowd, mentionably Sudhir, Sennur and Saquib for the many interesting discussions I had with them.

Dedication

To my mom and dad

Table of Contents

List of Figures

Chapter 1

Introduction

The *Signal to Interference Ratio* (SIR) is simply the ratio of the signal power S, to the interference power I. In this work we include the noise power N, in the interference power. So when we talk about SIR , it is the ratio $S/(I + N)$. The SIR is one of the parameters that gives a qualitative measure of the link performance. Several distributed algorithms for power control, handoff, diversity combining use the SIR to assess signal quality [2, 3, 8, 10, 14]. In CDMA cellular systems, power control is a crucial factor for satisfactory system performance. Several distributed algorithms for power control update power based on the SIR measurements [2, 8, 14]. It has been shown in [2] that power control based on SIR has the potential for a higher system performance than power control based on absolute signal strength measurements.

1.1 SIR Estimation

The algorithms mentioned above assume that the subscribers and/or the base stations have access to real time measurements of the received SIR. In reality, it can be quite difficult to obtain fast and accurate measurements of the SIR, hence practical resource allocation algorithms often use measurements of the total received power, i.e signal power plus interference plus noise power $(S + I + N)$ as a quality measure. However, the total received power is not a true indication of the link quality, because a high value of $(S + I + N)$ may not indicate a high $S/(I + N)$ ratio. The SIR estimation problem for analog (e.g. AMPS) cellular systems has been studied in [6, 12]. In [12], it has been shown that by separating the received signal into two components at different frequencies, where the two components are known by the receiver, it is possible to get an estimate of the SIR. The study in [6] is confined to systems employing QPSK modulation schemes. It has been demonstrated by numerical examples, that the average absolute difference between the in-phase and the quadrature envelopes are correlated to the SIR, and could, therefore, be used as an SIR estimator.

The methods above have focused on analog cellular systems, where the delay spread usually is negligible compared to the symbol duration. The second generation of cellular systems, e.g. D-AMPS (IS-136) and GSM, employ high bit rate TDMA schemes, resulting in time dispersive fading channels. SIR estimators for this type of systems have recently been studied in [1, 4, 5].

The study in [4] presents an estimation method, named Signal to Variation Power (SVR) estimator, which is based on the observation that on a short time scale, the signal from the desired transmitter will have a constant envelope, whilst the joint interference and noise signal produce oscillations. The SVR estimator has been applied to a DECT system in [5]. Numerical results reveal that the estimator suffers from a large bias for interesting values of the SIR.

Another SIR estimation method for TDMA cellular systems, has been developed in [1]. The algorithm is applied during the reception of the training sequence in each TDMA slot, in which case the receiver knows the transmitted sequence, providing an unbiased estimate of the SIR. The study in [1] has demonstrated by numerical examples, that the SIR can be estimated to within 2 dB in less than a second, when using the training and color code sequences in a D-AMPS cellular system. The method requires, though, some knowledge of the channel; however, in a fading environment, it is difficult to keep track of the channel variations.

1.2 Subspace based Techniques

To eliminate the necessity of requiring any knowledge about the channel, subspace based techniques for deriving fast algorithms that can provide accurate measurements in a highly mobile and fading environment have been studied in [9]. Subspace based techniques utilize the second order statistics of the observation vector to identify the signal subspace from the interference plus noise subspace. It was shown in [9] that for a GSM like system, the SIR could be estimated to within an error of 0.3 dB after only 200 ms, or within an error of 0.1 dB after only 0.6 seconds. This technique required practically no information about the channel. We propose to expand on these subspace based ideas for signal quality estimation in CDMA cellular systems.

1.3 Problem Description

As mentioned before, estimates of the SIR find application in a wide variety of algorithms aiming to combat the effects of cochannel interference. Surprisingly though, not much attention has been given to the estimation problem itself in CDMA cellular systems.For a generic CDMA cellular system this thesis develops a general SIR estimation technique , that is based on a signal subspace method using the sample covariance matrix of the received signal. The method requires essentially no information about the channel.

1.4 Objective of the Thesis

The sharing of the entire available bandwidth by the different users in a CDMA system results in a very different subspace structure (as compared to a TDMA system) for the covariance matrix of the observation vector. We show that the transmit filter, the channel, the matched filter and the sampler in a CDMA system can be represented by a discrete time transversal filter with a channel tap spacing equal to the symbol duration. The total received signal can, therefore, be modeled as consisting of a linear combination of the channel taps (the desired signal) added to the interference from other communication links and the receiver noise. Under the mild assumption that the users are transmitting their information independently of each other, the observation space, spanned by the columns of the sample covariance matrix, may be partitioned into a signal plus interference subspace and a noise subspace. The problem lies in extracting the signal only subspace from the interference plus signal subspace. We develop a matrix representation for the interference subspace, where it is shown that it can be represented by a *symmetric, positive definite tridiagonal matrix* i.e., the only non-zero elements in the matrix are on the main diagonal and the adjacent diagonals. Further, the off-diagonal terms of the interference matrix (for the case of random signature sequences such as those prescribed in [11]) are shown to be inversely proportional to the square of N, the processing gain. This would imply that as the signature sequences get longer, the interference appears increasingly white. With the help of this subspace decomposition, the power of the total received signal can easily be separated into the power of the desired signal and the interference plus noise power, yielding an efficient estimate of the SIR.

In Chapter 2, we introduce the model and describe our system. In Chapter 3, we derive the subspace based formulation for the SIR estimator method. We also look at a computationally efficient algorithm that tracks the signal subspace without doing an explicit eigenvalue decomposition. In Chapter 4, we derive analytical results on the accuracy of the eigenvalue decomposition based estimator. In Chapter 5, we evaluate the performance of both the proposed estimators in an hexagonal cellular system. Finally, we present our conclusions in Chapter 6.

Chapter 2

System Model

Consider an asynchronous CDMA system with $(K+1)$ users, where each user has a unique pseudorandom code sequence that is used to spread the information bits. If $s_j(t)$ is the waveform of user j, it is given by

$$s_j(t) = \sum_{k=0}^{N-1} c_j[k]\psi(t - kT_c) \tag{2.1}$$

where, $c_j[k] \in \{-1, 1\}$ is the k^{th} element of the spreading sequence for user j, $\psi(t)$ is the chip waveform, N is the processing gain. The chip duration T_c is related to the bit period T as $T_c = T/N$. We assume that $\psi(t)$ has unit energy and duration T_c. Let $\boldsymbol{h}_{ij}(t)$ represent the channel between user i and receiver j. This channel has multiple propagation paths, each of which has an associated attenuation factor and delay. The baseband channel impulse response which is the response of the channel at time t due to an impulse at time $t-\tau$, can be represented as a superposition of Dirac delta functions

$$\boldsymbol{h}_{ij}(\tau; t) = \sum_{p=1}^{M} h_{ijp}(t)\delta(\tau - \tau_{ijp}(t)), \tag{2.2}$$

where M is the effective number of channel taps, $h_{ijp}(t)$ is the complex valued attenuation weight for the p^{th} path, and $\tau_{ijp}(t)$ is the propagation delay for the p^{th} path. Figure 2.1 depicts the multipath channels between the various users and receiver 0. We assume that the channel parameters vary slowly with time, so that for sufficiently short intervals of time, the channel is approximately a linear time-invariant system

$$\boldsymbol{h}_{ij}(\tau) = \sum_{p=1}^{M} |h_{ijp}| e^{-j\theta_{ijp}} \delta(\tau - \tau_{ijp}) \tag{2.3}$$

The phase $\theta_{ijp} = \arg(h_{ijp})$ is assumed to be uniformly distributed between 0 and 2π. The tap delays, τ_{ijp} are modeled as independent uniform random variables over $[0, T]$.

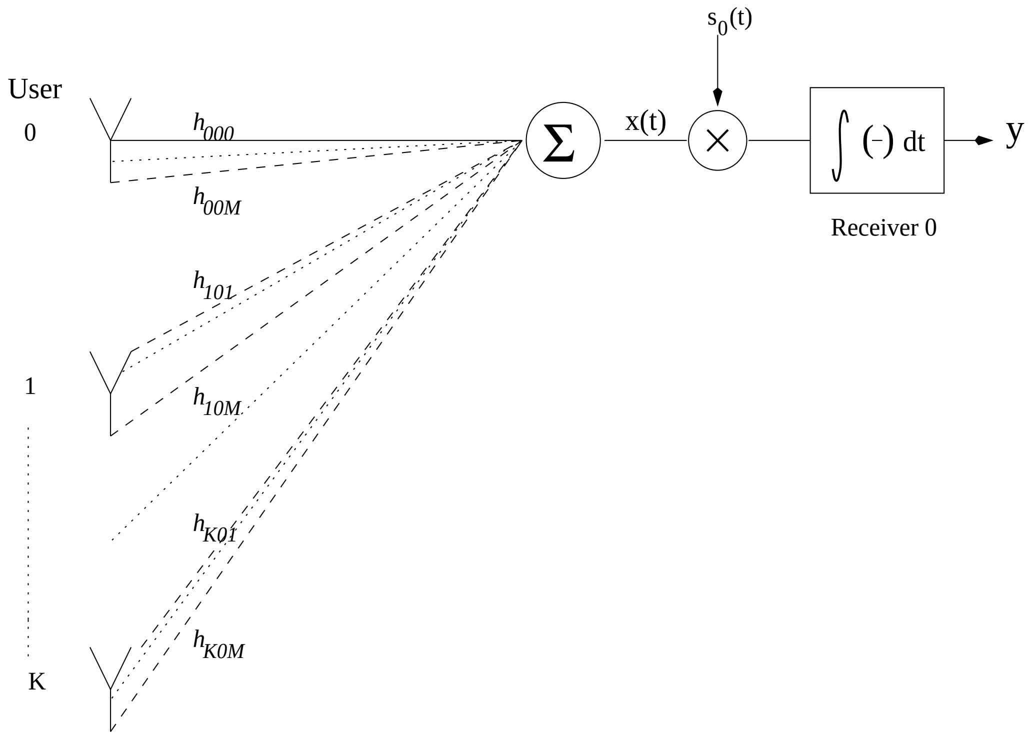

Figure 2.1: System model - Multipath channels between the various users and the receiver 0

Now, we will estimate the SIR of user 0 at receiver 0. For that, we require that user 0 transmit a known sequence of L bits called the *training sequence*, and we observe the output of receiver 0. Let $\boldsymbol{a}_0 = [a_{0,0}\ a_{0,1}\ \ldots\ a_{0,L-1}]^T$ denote the *training sequence* transmitted by user 0. Let $[\boldsymbol{a}_1\ \boldsymbol{a}_2,\ \ldots.\ \boldsymbol{a}_K]$ be the set of symbol sequences transmitted by the other K users.

The received signal at receiver 0 will then be sent through a filter matched to the code sequence of user 0. The output of this filter will be sampled every T units of time.

We assume that the dominant multipath of the user 0's signal is perfectly synchronized to the receiver 0. The various multipaths of the interference as well as the weak multipaths of user 0's signal are not synchronised with receiver 0 and arrive at receiver 0 with some offset delay. In general, the sampled received signal in the m^{th} interval will contain a part of the $(m-1)^{th}$ symbol as well as a part of the m^{th} symbol of each interfering user.

Figure 2.2 depicts the asynchronism in the system. The various constituents of the received signal in the m^{th} sampling interval are shown. If the received signal at receiver 0 is denoted by $x(t)$, it can be written as

$$\begin{aligned} x(t) &= \sum_{j=0}^{K}\sum_{p=1}^{M} h_{j0p} \sum_{m=0}^{L-1} a_{j,m-1} s_j(t-(m-1)T-\tau_{j0p}) \\ &+ \sum_{j=0}^{K}\sum_{p=1}^{M} h_{j0p} \sum_{m=1}^{L} a_{j,m} s_j(t-T-\tau_{j0p}) + n(t) \end{aligned} \quad (2.4)$$

Then, if we denote the output of the filter matched to $s_0(t)$, i.e. filter 0 as $\boldsymbol{y}$, the m^{th} element of $\boldsymbol{y}$ can be written as

$$\begin{aligned} y_m &= \sum_{j=0}^{K} a_{j,m-1} \sum_{p=1}^{M} \int_{mT}^{(m+1)T} s_0(t-mT)s_j(t-(m-1)T-\tau_{j0p})h_{j0p}dt \\ &+ \sum_{j=0}^{K} a_{j,m} \sum_{p=1}^{M} \int_{mT}^{(m+1)T} s_0(t-mT)s_j(t-mT-\tau_{j0p})h_{j0p}dt \\ &+ n_m \end{aligned} \quad (2.5)$$

where n_m is the component $m \geq 1$ of the noise vector. The observed vector $\boldsymbol{y}$ can be written compactly as

$$\boldsymbol{y} = (\boldsymbol{a}_0^l \boldsymbol{r}_{00}^l + \boldsymbol{a}_0^r \boldsymbol{r}_{00}^r)\boldsymbol{h}_{00} + \sum_{j=1}^{K} (\boldsymbol{a}_j^l \boldsymbol{r}_{j0}^l + \boldsymbol{a}_j^r \boldsymbol{r}_{j0}^r)\boldsymbol{h}_{j0} + \boldsymbol{n}, \quad (2.6)$$

where, $\boldsymbol{r}_{j0}^l = [r_{j01}^l \ r_{j02}^l \ . \ . \ . \ r_{j0M}^l]$, which represents the cross correlation between $s_0(t)$ and the left portion of $s_j(t)$ which is spreading the part of the previous bit contained in the sampling interval, and it is a function of the corresponding multipath delay. Specifically

$$r_{j0p}^l = \int_{mT}^{(m+1)T} s_0(t-mT)s_j(t-(m-1)T-\tau_{j0p})dt \quad (2.7)$$

A similar expression can be written for the cross correlation between $s_0(t)$ and the right portion of $s_j(t)$ as follows

$$r_{j0p}^r = \int_{mT}^{(m+1)T} s_0(t-mT)s_j(t-mT-\tau_{j0p})dt \quad (2.8)$$

If the first multipath of the user 0's signal is considered to be the dominant one, then since it is perfectly synchronized to the receiver, $r_{001}^r = 1$ and $r_{001}^l = 0$. The vector of channel taps in (2.6) is given as

$$\boldsymbol{h}_{ij} = [h_{ij1} \ h_{ij2} \ . \ . \ . \ h_{ijM}]^T, \quad (2.9)$$

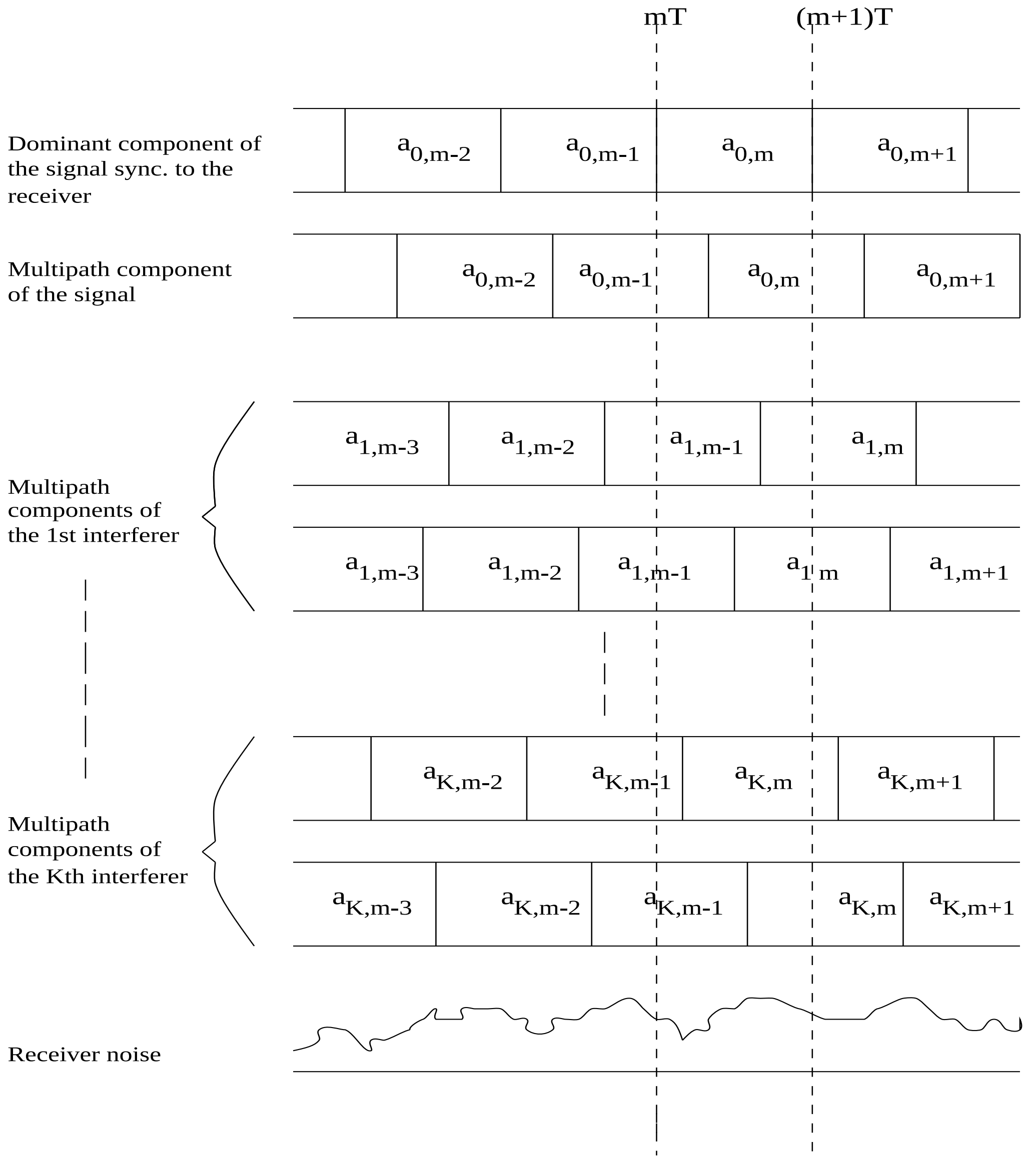

Figure 2.2: Asynchronous CDMA System

and the transmitted symbols due to the interferers are

$$\boldsymbol{a}_j^r = [a_{j,0}\ a_{j,1}\ a_{j,2}\ \dots\ a_{j,L-1}]^T \tag{2.10}$$

$$\boldsymbol{a}_j^l = [a_{j,-1}\ a_{j,0}\ a_{j,1}\ \dots\ a_{j,L-2}]^T \tag{2.11}$$

The receiver noise $\boldsymbol{n}$ is modeled as an independent zero-mean, complex Gaussian random process with second order moments

$$E[\boldsymbol{n}(k)\boldsymbol{n}^H(l)] = \sigma_N^2 \boldsymbol{I}\delta_{kl} \quad ; \quad E[\boldsymbol{n}(k)\boldsymbol{n}^T(l)] = 0, \tag{2.12}$$

where $\boldsymbol{x}^H$ denotes the Hermitian transpose of $\boldsymbol{x}$, σ_N^2 is the noise power, δ_{lk} represents the Kronecker delta function, and $\boldsymbol{I}$ is the identity matrix. Note here that we have assumed that the channel taps do not vary over L symbols.

We assume that the received bits from the interferers are uncorrelated and mutually uncorrelated, i.e., $E[a_{j,m}a_{j,n}] = E[a_{j,m}]E[a_{j,n}] = 0, \text{for all } m \neq n, \text{and } j,k = 1,2...K$. The channel taps of the various users are assumed to be uncorrelated as well. Therefore, $E[h_{j0m}h_{j0n}] = 0, \text{for all } m \neq n$. Note that this assumption holds when the impulse response $\boldsymbol{h}_{ij}(t)$ is modeled as a zero-mean complex random process, in which case the envelope $|\boldsymbol{h}_{ij}(t)|$ at any instant is Rayleigh distributed [17]. In the event that there are fixed scatterers in the medium in addition to randomly moving scatterers; $\boldsymbol{h}_{ij}(t)$ can no longer be modeled as having zero-mean. In that case, the envelope $|\boldsymbol{h}_{ij}(t)|$ has a Rice distribution and the channel is said to be a Ricean fading channel. Another probability distribution that has been used to model the envelope of fading signals is the Nakagami-m distribution [17]. Here, we assume our channel to be Rayleigh fading.

We now focus our attention on the covariance matrix $\boldsymbol{R}$, of the observation vectors, that will be used to derive the subspace based SIR estimator. The matrix $\boldsymbol{R}$ can be expressed as

$$\begin{aligned} \boldsymbol{R} &= E[\boldsymbol{y}\boldsymbol{y}^H] \\ &= \boldsymbol{R}_S + \boldsymbol{R}_I + \boldsymbol{R}_N, \end{aligned} \tag{2.13}$$

where the above decomposition follows from the assumption of uncorrelated users. In

(2.13), the signal covariance matrix $\boldsymbol{R}_S$ is given by

$$\boldsymbol{R}_S = E[(\boldsymbol{a}_0^l \boldsymbol{r}_{00}^l + \boldsymbol{a}_0^r \boldsymbol{r}_{00}^r)\boldsymbol{h}_{00}\boldsymbol{h}_{00}^H(\boldsymbol{r}_{00}^{lH}\boldsymbol{a}_0^{lH} + \boldsymbol{r}_{00}^{rH}\boldsymbol{a}_0^{rH})] \tag{2.14}$$

The matrix $\boldsymbol{R}_S$ is in general a matrix of some rank $d \leq L$. As an illustration let us look at a case when d would be equal to 1. For perfect synchronization, $\boldsymbol{r}_{00}^r = [1 \dots 1]$, $\boldsymbol{r}_{00}^l = [0 \dots 0]$. Then,

$$\begin{aligned} \boldsymbol{R}_S &= E[\boldsymbol{a}_0 \boldsymbol{r}_{00}^r \boldsymbol{h}_{00}\boldsymbol{h}_{00}^H \boldsymbol{r}_{00}^r \boldsymbol{a}_0^H] \\ &= \boldsymbol{a}_0 \boldsymbol{r}_{00}^r E[\boldsymbol{h}_{00}\boldsymbol{h}_{00}^H]\boldsymbol{r}_{00}^{rH}\boldsymbol{a}_0 H \end{aligned} \tag{2.15}$$

On account of the assumption about the channel taps being mutually uncorrelated, $E[\boldsymbol{h}_{00}\boldsymbol{h}_{00}^H]$ is a diagonal matrix. Hence, $\boldsymbol{r}_{00}^r E[\boldsymbol{h}_{00}\boldsymbol{h}_{00}^H]\boldsymbol{r}_{00}^{rH} = \sum_{p=1}^M h_{00p}^2$. Thus, $\boldsymbol{R}_S = (\sum_{p=1}^M h_{00p}^2)\boldsymbol{a}_0\boldsymbol{a}_0^H$, which a matrix of rank $d = 1$.

The matrix $\boldsymbol{R}_N$ in (2.13) is the noise covariance matrix given by

$$\boldsymbol{R}_N = \sigma_N^2 \boldsymbol{I}. \tag{2.16}$$

The matrix $\boldsymbol{R}_I$ in (2.13) is the interference covariance matrix given by

$$\boldsymbol{R}_I = E\left[\sum_{j=1}^{K}(\boldsymbol{a}_j^l \boldsymbol{r}_{j0}^l + \boldsymbol{a}_j^r \boldsymbol{r}_{j0}^r)\boldsymbol{h}_{j0}\sum_{i=1}^{K}\boldsymbol{h}_{i0}^H(\boldsymbol{r}_{i0}^{lH}\boldsymbol{a}_i^{lH} + \boldsymbol{r}_{i0}^{rH}\boldsymbol{a}_i^{rH})\right] \tag{2.17}$$

The matrix $\boldsymbol{R}_I$ can be written as

$$\boldsymbol{R}_I = \begin{pmatrix} \alpha & \beta & 0 & \cdots & 0 \\ \beta & \alpha & \beta & \cdots & 0 \\ 0 & \beta & \alpha & \ddots & \\ \vdots & & \ddots & \ddots & \beta \\ 0 & \cdots & \cdots & \beta & \alpha \end{pmatrix}, \tag{2.18}$$

which is a tridiagonal, symmetric, positive definite matrix with elements α and β given as

$$\alpha = \sum_{j=1}^{K}\sum_{p=1}^{M} E[(r_{j0p}^r)^2 + (r_{j0p}^l)^2] \cdot E[h_{j0p}h_{j0p}^H] \tag{2.19}$$

$$\beta = \sum_{j=1}^{K}\sum_{p=1}^{M} E[r_{j0p}^r r_{j0p}^l] \cdot E[h_{j0p}h_{j0p}^H] \tag{2.20}$$

Denoting $E[h_{j0p}h_{j0p}^H] = \sigma^2_{h_{j0p}}$, the terms in $\boldsymbol{R}_I$ can be further simplified under the assumption that the code sequences of the various interferers are uncorrelated psuedo-random sequences, as

$$\alpha = (\sum_{j=1}^{K}\sum_{p=1}^{M}\sigma^2_{j0p})\left(\frac{2}{3N}+\frac{1}{3N^2}\sum_{k=1}^{N-1}c_0[k]c_0[k+1]\right) \tag{2.21}$$

$$\beta = (\sum_{j=1}^{K}\sum_{p=1}^{M}\sigma^2_{j0p})\left(\frac{1}{6N^2}c_0[1]c_0[N]\right) \tag{2.22}$$

The details of the above derivation are shown in Appendix A. It is seen from (2.22) that the off-diagonal terms $\beta \longrightarrow 0$, as N becomes large, since in any practical system, the number of interferers, $K \ll N^2$. Note that the total interference power, σ_I^2 is given by

$$\begin{aligned} \sigma_I^2 &= \sum_{j=1}^{K}\sum_{p=1}^{M} E[(r^r_{j0p}+r^l_{j0p})^2]\cdot E[h_{j0p}h^H_{j0p}] \\ &= \alpha + 2\beta \end{aligned} \tag{2.23}$$

We can rewrite $\boldsymbol{R}_I$ as

$$\boldsymbol{R}_I = \alpha\boldsymbol{I} + \beta\boldsymbol{T} \tag{2.24}$$

where $\boldsymbol{T}$ is given by

$$\boldsymbol{T} = \begin{pmatrix} 0 & 1 & 0 & \cdots & 0 \\ 1 & 0 & 1 & \cdots & 0 \\ 0 & 1 & 0 & \ddots & \\ \vdots & & \ddots & \ddots & 1 \\ 0 & \cdots & \cdots & 1 & 0 \end{pmatrix}, \tag{2.25}$$

For large N , β is found to be negligible, $\boldsymbol{R}_I$ is approximately diagonal, with the diagonal elements equal to the interference power σ_I^2. Hence we can write

$$\boldsymbol{R}_I \approx \sigma_I^2\boldsymbol{I} \tag{2.26}$$

Note that if we had synchronous transmission, i.e. if all the users were perfectly synchronised to user 0's receiver, then $\boldsymbol{R}_I$ would be diagonal. The non-diagonal nature of the interference covariance matrix is a result of the asynchronism in the system - the energy of each interfering bit is spread over two consecutive sampling intervals. The tridiagonal nature of the interference covariance matrix arises from the fact that we considered the maximum offset delay of the transmitted bit sequence of the interferers to be one bit with respect to the training sequence. This is a reasonable assumption, but in the general case where the maximum offset is more than one bit, we would have non-zero terms in the corresponding off-diagonals as well. Then the matrix would no longer be tridiagonal. But as has been shown above, these terms would approach zero for large N. Hence in any case for a large processing gain, $\boldsymbol{R}_I$ would be approximately diagonal, with the diagonal elements equal to the interference power.

Chapter 3

Subspace Based SIR estimator

3.1 SIR Estimation using Eigenvalue Decomposition (ED)

Given the above formulation for the covariance matrix $\boldsymbol{R}$, we now use a subspace based approach to arrive at the SIR estimator. To estimate the SIR, we need to separate the desired signal and the interference plus noise signal from the observation vector. In order to separate the signal covariance matrix from the interference plus noise covariance matrix we require the interference plus noise covariance matrix to be proportional to the identity matrix. Following the discussion of Chapter 2, we see that $\boldsymbol{R}$ can be written as

$$\begin{aligned}\boldsymbol{R} &= \boldsymbol{R}_S + \boldsymbol{R}_I + \boldsymbol{R}_N \\ &= \boldsymbol{R}_S + \alpha \boldsymbol{I} + \beta \boldsymbol{T} + \sigma_N^2 \boldsymbol{I} \\ &= \boldsymbol{R}_S + \beta \boldsymbol{T} + (\sigma_I^2 - 2\beta + \sigma_N^2)\boldsymbol{I} \\ &= \tilde{\boldsymbol{R}}_S + \tilde{\sigma}_{I+N}^2 \boldsymbol{I} \end{aligned} \tag{3.1}$$

Here, $\tilde{\boldsymbol{R}}_S = \boldsymbol{R}_S + \beta \boldsymbol{T}$ and $\tilde{\sigma}_{I+N}^2 = (\sigma_I^2 - 2\beta + \sigma_N^2) = (\sigma_{I+N}^2 - 2\beta)$.

The signal covariance matrix $\boldsymbol{R}_S$ is a matrix of some rank d. The rank of $\tilde{\boldsymbol{R}}_S$ would in general be different from the rank of $\boldsymbol{R}_S$. As we have already pointed out in Chapter 2, for large processing gain, the value of β is negligible leaving us with $\tilde{\boldsymbol{R}}_S \approx \boldsymbol{R}_S$ and $\tilde{\sigma}_{I+N}^2 \approx \sigma_{I+N}^2$. Also for negligible β there is no significant change in the value of d and the eigenvalues of $\tilde{\boldsymbol{R}}_S$ would be approximately the same as those of $\boldsymbol{R}_S$.

Now, to separate the signal and interference subspaces, do an eigenvector decomposition of $\boldsymbol{R}$. The matrix $\boldsymbol{R}$ can be expressed in terms of its eigenvector decomposition

$$\boldsymbol{R} = \boldsymbol{U}\boldsymbol{\Sigma}\boldsymbol{U}^H, \tag{3.2}$$

where $\boldsymbol{U} = [\boldsymbol{e}_1 \ \ldots \ \boldsymbol{e}_L]$ consists of the orthonormal eigenvectors of $\boldsymbol{R}$. The diagonal matrix, $\boldsymbol{\Sigma}$ =diag(λ_i), contains the corresponding eigenvalues, where $\lambda_1 \geq \lambda_2 \geq \ldots \geq \lambda_L$. The eigenvalues of $\boldsymbol{R}$ have the following structure [20]

$$\lambda_i = \begin{cases} \sigma_{S_i}^2 + \sigma_{I+N}^2 \ , & \text{if } \ 1 \leq i \leq d \\ & \\ \sigma_{I+N}^2 \ , & d+1 \leq i \leq L \end{cases} , \tag{3.3}$$

where $\sigma_{S_i}^2$ is the power (variance) of the desired signal along the i^{th} eigenvector. From (3.3), we realize that the d largest eigenvalues in $\boldsymbol{\Sigma}$ correspond to the signal subspace. Further from the results shown in the previous chapter, the interference covariance matrix $\boldsymbol{R}_I$ is almost diagonal. Thus, if we know the dimension d, then the signal subspace can be identified. Then, using (3.3), we can obtain the powers of the desired signal and the interference plus noise, respectively. This is the basic idea underlying our estimation technique.

The true covariance matrix $\boldsymbol{R}$ is of course not known and has to be estimated. Since we want to track time variations of the SIR, we form a *moving average* or *Bartlett* estimate of the covariance matrix from the J most recent observation vectors. Let $\boldsymbol{y}(k)$ denote the k^{th} observation vector. Suppose we wish to obtain an estimate of the SIR after the n^{th} observation vector. Then we have

$$\hat{\boldsymbol{R}}(n) = \frac{1}{J} \sum_{k=n-J+1}^{n} \boldsymbol{y}(k)(\boldsymbol{y}(k))^H \tag{3.4}$$

Here, $\hat{\boldsymbol{R}}(n)$ is the *sample covariance matrix.* Its properties have briefly been stated in Appendix B. It has been shown, e.g. [16], that the eigenvalues of the sample covariance matrix in (3.4) is a maximum likelihood estimate of the eigenvalues of the true covariance matrix $\boldsymbol{R}$.

Almost all existing approaches to the determination of the dimension of the signal subspace are based on the observation that the smallest eigenvalue of the covariance matrix has multiplicity $L-d$. A variety of tests exist to determine the signal space dimension d. We comment here on the common approaches:

1. Extended Sphericity Test

   This is a sequence of likelihood ratio tests for equality of the $L-d$ smallest eigenvalues of the estimated covariance matrix. This classical test has been described in [15]. The resulting test statistic for the signal subspace of dimension d is

$$T_{sph} = \frac{\left[(L-d)^{-1}\sum_{i=d+1}^{L}\lambda_i\right]}{\left(\prod_{i=d+1}^{L}\lambda_i)^{1/(L-d)}\right)} \tag{3.5}$$

   where $\lambda_i,\ i=1,2,...,L$, denote the eigenvalues of the estimated covariance matrix in descending order. The target number is found with T_{sph} by testing the equality of the smallest eigenvalues. This is done by comparing the arithmetic and geometric mean of these eigenvalues. The problem with this test is that the test statistic is complicated. Therefore, to obtain the approximate error level, different χ^2- approximations have been suggested in the statistical literature. For small sample sizes, these asymptotic approximations do not have satisfactory properties.

2. Information Theoretic Tests

   The most popular criteria are the AIC (An Information Criterion) , and the MDL (Minimum Descriptive Length) principles. The two criteria estimate the dimension of the signal space by respectively minimizing the function

$$F_{\mathrm{AIC}}(m) = J(L-m)\log[T_{sph}(m)] + m(2L-m) \tag{3.6}$$

   and

$$F_{\mathrm{MDL}}(m) = J(L-m)\log[T_{sph}(m)] + \frac{1}{2}m(2L-m)log(J) \tag{3.7}$$

   We observe that these criteria are based on different approximations for the distribution of the extended sphericity test statistic. We have tested both these criteria and for our application, both the criteria achieved satisfactory performance. The MDL criterion has been found to obtain superior performance in some cases [9].

   Strong consistency of the MDL method has been proven in [23]. Hence after obtaining the MDL objective function, $F_{\mathrm{MDL}}(m)$ the signal space dimension is estimated as [18]

$$\hat{d} = \arg\min_{m} F_{\mathrm{MDL}}(m) \ . \tag{3.8}$$

Using (3.2),(3.3) (3.4) and (3.8) we propose the following subspace based SIR estimation algorithm.

Subspace Based SIR Estimator using ED

(1) Make an eigenvector decomposition of the sample covariance matrix $\hat{\boldsymbol{R}}$

$$\hat{\boldsymbol{R}} = \hat{\boldsymbol{U}}\hat{\boldsymbol{\Sigma}}\hat{\boldsymbol{U}}^H,$$

where $\hat{\boldsymbol{\Sigma}} = \mathrm{diag}(\hat{\lambda}_i)$, with $\hat{\lambda}_1 > \ldots > \hat{\lambda}_L$.

(2) Estimate the current dimension of the signal subspace, $\hat{d}$, using (3.5),(3.7) and (3.8).

(3) Estimate the interference power according to

$$\hat{\sigma}^2_{I+N} = \frac{1}{L-\hat{d}} \sum_{j=\hat{d}+1}^{L} \hat{\lambda}_j \ ,$$

and the signal power according to

$$\hat{\sigma}^2_S = (\sum_{j=1}^{\hat{d}} \hat{\lambda}_j) - \hat{d}\,\hat{\sigma}^2_{I+N} \ .$$

(4) The estimate of the SIR is then obtained as

$$\hat{\gamma} = \frac{1}{L}\frac{\hat{\sigma}^2_S}{\hat{\sigma}^2_{I+N}} \ , \tag{3.9}$$

where the factor $1/L$ accounts for the fact that we have L samples (symbols) of the received signal within each observation vector.

In the next chapter we derive analytical results for the performance of the ED based SIR estimator.

Choose $c_j(0)$ and $\boldsymbol{w}_j(0)$
FOR $t = 1, 2, \ldots$ DO
$\quad \boldsymbol{y}(t)$: Current data vector
$\quad \boldsymbol{v}_1(t) = \boldsymbol{y}(t)$
$\quad$ FOR $j = 1, \ldots d$ DO
$\qquad x_j(t) = \boldsymbol{w}_j^H(t-1)\boldsymbol{v}_j(t)$
$\qquad c_j(t) = \beta c_j(t-1) + \lvert x_j(t)\rvert^2$
$\qquad \boldsymbol{e}_j(t) = \boldsymbol{v}_j(t) - \boldsymbol{w}_j(t-1)x_j(t)$
$\qquad \boldsymbol{w}_j(t) = \boldsymbol{w}_j(t-1) + \boldsymbol{e}_j(t)[x_j^*(t)/c_j(t)]$
$\qquad \boldsymbol{v}_{j+1}(t) = \boldsymbol{v}_j(t) - \boldsymbol{w}_j(t)x_j(t)$

Table 3.1: The PASTd algorithm for tracking the signal subspace

3.2 Subspace tracking using the PASTd algorithm

The ED estimator described in the previous section is based on eigenvector decomposition which is a computationally intensive task. In the context of a constantly varying channel, the ED estimator may be unsuitable for tracking the SIR. A number of adaptive algorithms for subspace tracking have been developed in the past. Most of these methods can be grouped into three families. In the first one, classical batch ED/SVD methods like the QR algorithm, Jacobi rotation and the power iteration have been modified for use in adaptive processing [25] - [28]. In the second family, variations of Bunch's rank-one updating algorithm [29] have been proposed. The third class of algorithms considers the ED/SVD as a constrained or unconstrained optimization problem. In the work by Yang [24], the signal subspace has been shown to be the solution of an unconstrained minimization problem. Let $\boldsymbol{x}$ be a complex valued random vector process with correlation matrix $\boldsymbol{R}$. Consider the following scalar function

$$\begin{aligned} J(\boldsymbol{W}) &= E\left[\| \boldsymbol{x} - \boldsymbol{W}\boldsymbol{W}^H\boldsymbol{x} \|^2\right] \\ &= \mathrm{tr}(\boldsymbol{R}) - 2\mathrm{tr}(\boldsymbol{W}^H\boldsymbol{R}\boldsymbol{W}) + \mathrm{tr}(\boldsymbol{W}^H\boldsymbol{R}\boldsymbol{W} \cdot \boldsymbol{W}^H\boldsymbol{W}) \qquad (3.10) \end{aligned}$$

with a matrix argument $\boldsymbol{W} \in C^{n\times d}$ with $d < n$. Here, $\mathrm{tr}(\cdot)$ is an abbreviation for the trace. In [24] it was proven that $J(\boldsymbol{W})$ has a global minimum at which the column space of $\boldsymbol{W}$ equals the signal subspace. At each stationary point of

$J(\boldsymbol{W})$, it equals the sum of the eigenvalues of those eigenvectors which are not involved in the signal subspace. All sample vectors available in the time interval $1 \leq t \leq n$ are involved in estimating the signal subspace at the time instant n. So, if $\boldsymbol{y}(n)$ is the data input at the n^{th} instant, the cost function to be minimized is,

$$J(\boldsymbol{W}(n)) = \sum_{t=1}^{n} \beta^{n-t} \parallel \boldsymbol{y}(t) - \boldsymbol{W}(n)\boldsymbol{W}^{H}(n)\boldsymbol{y}(t) \parallel^{2} \qquad (3.11)$$

where β is a forgetting factor meant to downweigh the past observations. The function $J(\boldsymbol{W})$ is a fourth order function of the elements of $\boldsymbol{W}$. Iterative algorithms are thus necessary to minimize $J(\boldsymbol{W})$.

The PASTd algorithm has been summarised in Table 3.1. Here, as before, d is the signal subspace dimension and it is assumed to be known. Also, $\boldsymbol{w}_j(t)$, $j = 1 \ldots d$ are columns of the matrix $\boldsymbol{W}(t)$, and a simple initial choice for these columns would be the d leading unit vectors of the $L \times L$ identity matrix, where L is the dimension of the input data vector $\boldsymbol{y}$. Note that the PASTd algorithm allows for explicit computation of the eigencomponents. To be specific, $\boldsymbol{w}_j(t)$ is an estimate of the j^{th} eigenvector of the covariance matrix $\boldsymbol{C}(t)$ and $c_j(t)$ is an estimate of the corresponding eigenvalue at time t. Thus, $c_j(t) = \hat{\sigma}^2_{S_j}$ for $j = 1, \ldots d$. The key issue of this approach is to approximate $\boldsymbol{W}^H(n)\boldsymbol{y}(t)$ in (3.11) by the expression

$$\boldsymbol{x}(t) = \boldsymbol{W}^{H}(t-1)\boldsymbol{y}(t) \qquad (3.12)$$

This results in the modified cost function

$$J^{'}(\boldsymbol{W}(n)) = \sum_{t=1}^{n} \beta^{n-t} \parallel \boldsymbol{y}(t) - \boldsymbol{W}(n)\boldsymbol{x}(t) \parallel^{2} \qquad (3.13)$$

The difference between $\boldsymbol{W}^H(n)\boldsymbol{y}(t)$ and $\boldsymbol{W}^H(t-1)\boldsymbol{y}(t)$ is small, particularly when t is close to n. The updating of the columns of the $\boldsymbol{W}(t)$ matrix has been indicated in step 4 of the table, where $\boldsymbol{e}(t)$ is an estimator of the gradient of $\boldsymbol{J}^{'}$ w.r.t. $\boldsymbol{W}(t)$. The last equation in the table denotes the deflation technique. The basic idea of the deflation technique is the sequential estimation of the principal components [33], [34]. First, the most dominant eigenvector is updated using the algorithm with $d = 1$. Then we remove the projection of the current data vector $\boldsymbol{y}(t)$ onto this eigenvector from $\boldsymbol{y}(t)$ itself. Now since the second dominant eigenvector becomes the most dominant one in the updated data vector (represented by the dummy variable $\boldsymbol{v}(t)$), it can be extracted in the same way as before. Applying this procedure repeatedly, all desired eigencomponents are estimated sequentially. And since $J^{'}(\boldsymbol{W}_n)$ equals the sum of the noise plus interference eigenvalues at its minimun, we can use it as an estimate of the same, i.e, $(L-d)\hat{\sigma}^2_{I+N}$. The complexity of the PASTd algorithm is $4Ld+O(d)$ operations per update. This is a much lower complexity compared to the ED estimator, since no matrix inversion operations are involved.

Chapter 4

Analysis of the ED Estimator

In order to derive analytical expressions for the accuracy of the ED estimator described in the previous chapter, we need the following preliminaries. Consider the problem of estimating the covariance matrix of an $m-$variate normal distribution $N_m(\boldsymbol{\mu}, \boldsymbol{C})$, where, $\boldsymbol{\mu}$ is the mean and $\boldsymbol{C}$ is the covariance matrix of the distribution. In this case, the sample covariance matrix $\boldsymbol{S}$ formed from n random vectors $\boldsymbol{X}_1 \ \dots \ \boldsymbol{X}_n$ has m distinct eigenvalues $l_1 > \ \dots \ > l_m$ which are estimates of the eigenvalues $\lambda_1 \geq \ \dots \ \geq \lambda_m$ of $\boldsymbol{C}$ [16]. Then, it has been shown by Lawley [21] that if λ_i is a distinct eigenvalue of $\boldsymbol{C}$, then the mean and variance of l_i can be expanded for large n, where n is the number of samples, as

$$E(l_i) = \lambda_i + \frac{\lambda_i}{n} \sum_{j=1, j\neq i}^{m} \frac{\lambda_j}{\lambda_i - \lambda_j} + O(n^{-2}) \tag{4.1}$$

and

$$\mathrm{Var}(l_i) = \frac{2\lambda_i^2}{n} \left[1 - \frac{1}{n} \sum_{j=1, j\neq i} (\frac{\lambda_j}{\lambda_i - \lambda_j})^2 \right] + O(n^{-3}) \tag{4.2}$$

We propose to use the above result for analyzing the accuracy of the SIR estimator. The eigenvalue estimation of the covariance matrix $\boldsymbol{R}$ is equivalent to a sample estimate based on samples from an $L-$variate normal distribution $N_L(\boldsymbol{0}, \boldsymbol{R})$.

The matrix $\boldsymbol{R}$ has $(d+1)$ distinct eigenvalues, specifically, $\lambda_i = \sigma_{S_i}^2 + \sigma_{I+N}^2$ for $i = 1, \dots d$ and $\lambda_{d+1} = \sigma_{I+N}^2$. The eigenvalue λ_{d+1} is a repeated eigenvalue of multiplicity $L - d$. Note that the eigenvalues λ_i, $i = 1 \dots d$ can be written as $\lambda_i = \sigma_{S_i}^2 + \lambda_{d+1}$. Also let us denote $\gamma_i = \frac{\sigma_{S_i}^2}{\sigma_{I+N}^2}$. Then, we can write

$$\lambda_i = \lambda_{d+1}(\gamma_i + 1) \qquad i = 1 \dots d. \tag{4.3}$$

Hence, if $\hat{\boldsymbol{R}}$ is the sample covariance matrix, with eigenvalues $\hat{\lambda}_1 \ldots \hat{\lambda}_L$, we can simplify (4.1) to write

$$E(\hat{\lambda}_i) = \lambda_{d+1}\left[\gamma_i + 1 + \frac{\gamma_i+1}{n}\left(\sum_{j=1,j\neq i}^{L}\frac{\gamma_j+1}{\gamma_i-\gamma_j} + \frac{L-d}{\gamma_i}\right)\right],\ \forall\, i = 1 \ldots d \quad (4.4)$$

and

$$E(\hat{\lambda}_{d+1}) = \lambda_{d+1}\left[1 - \frac{1}{n} - \frac{1}{n}\sum_{i=1}^{d}\frac{1}{\gamma_i}\right], \quad (4.5)$$

Note that the true SIR is $\gamma = \frac{1}{L}\sum_{i=1}^{d}\gamma_i$. From (3.9), the estimated SIR is

$$\hat{\gamma} = \frac{1}{L}\left(\frac{\sum_{i=1}^{d}(\hat{\lambda}_i - \hat{\lambda}_{d+1})}{\hat{\lambda}_{d+1}}\right) \quad (4.6)$$

Therefore, the expression for the expected value of the estimated SIR is

$$\begin{aligned} E(\hat{\gamma}) &= \frac{1}{L}E\left(\frac{\sum_{i=1}^{d}(\hat{\lambda}_i - \hat{\lambda}_{d+1})}{\hat{\lambda}_{d+1}}\right) \\ &= \frac{1}{L}E\left(\frac{\sum_{i=1}^{d}\hat{\lambda}_i}{\hat{\lambda}_{d+1}}\right) - \frac{d}{L} \\ &\approx \frac{1}{L}\sum_{i=1}^{d}E(\hat{\lambda}_i)E\left(\frac{1}{\hat{\lambda}_{d+1}}\right) - \frac{d}{L} \quad (4.7) \end{aligned}$$

Note that in (4.7) we are making the assumption that the $\hat{\lambda}_i$'s and $\hat{\lambda}_{d+1}$ are independent random variables. We will validate the analysis based on this assumption through numerical results in the next chapter. Now, if f is a convex function and X is some random variable, then Jensen's inequality states that

$$E[f(X)] \geq f(E[X]) \quad (4.8)$$

Now, for strictly non-negative X, the function $f = 1/X$ is a convex function. Since the eigenvalues of the sample covariance matrix are all strictly non-negative, we can apply Jensen's inequality and rewrite (4.7) as

$$E(\hat{\gamma}) \geq \frac{1}{L}\frac{E(\sum_{i=1}^{d}\hat{\lambda}_i)}{E(\hat{\lambda}_{d+1})} - \frac{d}{L} \quad (4.9)$$

Let us evaluate these bounds for the case when $d = 1$. This is when we consider the weak multipaths of the signal as interference and ignore them. In this case, the matrix $\boldsymbol{R}$, has 2 distinct eigenvalues, specifically, $\lambda_1 = L\sigma_S^2 + \sigma_{I+N}^2$ and

$\lambda_2 = \sigma^2_{I+N}$. The eigenvalue λ_2 is a repeated eigenvalue of multiplicity $(L-1)$. For this case, it follows from (4.4) and (4.5) that

$$E(\hat{\lambda}_1) = \lambda_2 \left[L\gamma + 1 + \frac{1}{n} + \frac{1}{nL\gamma}\right] \tag{4.10}$$

$$E(\hat{\lambda}_2) = \lambda_2 \left[1 - \frac{1}{n} - \frac{1}{nL\gamma}\right] \tag{4.11}$$

Using (4.9), (4.10) and (4.11) we can further write

$$E(\hat{\gamma}) \geq \gamma + \gamma \left(\frac{L^2 + \frac{3L}{\gamma} + \frac{2}{\gamma^2}}{(n-1)L^2 - \frac{L}{\gamma}}\right) \tag{4.12}$$

We now formulate the fractional error in the SIR estimate as

$$\begin{aligned} e &= \left(\frac{E(\hat{\gamma}) - \gamma}{\gamma}\right) \\ &\geq \frac{L^2 + \frac{3L}{\gamma} + \frac{2}{\gamma^2}}{(n-1)L^2 - \frac{L}{\gamma}} \end{aligned} \tag{4.13}$$

Thus we get lower bounds on the estimator mean and fractional error. We now wish to derive a similar bound on the variance of the above estimator. We simplify (4.2) to write

$$\mathrm{Var}(\hat{\lambda}_1) = \frac{2}{n}\lambda_2^2 (L\gamma + 1)^2 \left(1 - \frac{1}{n(L\gamma)^2}\right) \tag{4.14}$$

$$\mathrm{Var}(\hat{\lambda}_2) = \frac{2}{n}\lambda_2^2 \left(1 - \frac{(L\gamma + 1)^2}{n(L\gamma)^2}\right) \tag{4.15}$$

Now from (4.6)

$$\hat{\gamma} = \frac{1}{L}\left(\frac{\hat{\lambda}_1}{\hat{\lambda}_2} - 1\right) \tag{4.16}$$

The variance of $\hat{\gamma}$ can be written as

$$\mathrm{Var}(\hat{\gamma}) = \mathrm{Var}(\frac{1}{L}\frac{\hat{\lambda}_1}{\hat{\lambda}_2} - \frac{1}{L}) = \frac{1}{L^2}\mathrm{Var}\left(\frac{\hat{\lambda}_1}{\hat{\lambda}_2}\right) \tag{4.17}$$

Consider

$$\mathrm{Var}\left(\frac{\hat{\lambda}_1}{\hat{\lambda}_2}\right) = E\left[\left(\frac{\hat{\lambda}_1}{\hat{\lambda}_2}\right)^2\right] - E^2\left(\frac{\hat{\lambda}_1}{\hat{\lambda}_2}\right) \tag{4.18}$$

Again using the assumption that $\hat{\lambda}_1$ and $\hat{\lambda}_2$ are independent random variables, we can write

$$\begin{aligned} \mathrm{Var}\left(\frac{\hat{\lambda}_1}{\hat{\lambda}_2}\right) &= E(\hat{\lambda}_1^2)E\left(\frac{1}{\hat{\lambda}_2^2}\right) - E^2(\hat{\lambda}_1)\cdot E^2\left(\frac{1}{\hat{\lambda}_2}\right) \\ &\geq \mathrm{Var}(\hat{\lambda}_1)\cdot E^2\left(\frac{1}{\hat{\lambda}_2}\right) \end{aligned} \tag{4.19}$$

where we have used the fact that

$$\mathrm{Var}\left(\frac{1}{\hat{\lambda}_2}\right) = E\left(\frac{1}{\hat{\lambda}_2^2}\right) - E^2\left(\frac{1}{\hat{\lambda}_2}\right) \geq 0 \tag{4.20}$$

Now, by Jensen's inequality, we get

$$E\left(\frac{1}{\hat{\lambda}_2}\right) \geq \frac{1}{E(\hat{\lambda}_2)} \tag{4.21}$$

This implies that

$$\mathrm{Var}\left(\frac{\hat{\lambda}_1}{\hat{\lambda}_2}\right) \geq \frac{\mathrm{Var}(\hat{\lambda}_1)}{E^2(\hat{\lambda}_2)} \tag{4.22}$$

Using (4.14),(4.15) and (4.22) we get lower bound on the variance of the estimator,

$$\mathrm{Var}(\hat{\gamma}) \geq \frac{2(L\gamma+1)^2(n(L\gamma)^2-1)}{(L\gamma(n-1)-1)^2} \tag{4.23}$$

It can be seen that as $n \longrightarrow \infty$, the lower bound on the variance of the estimator $\longrightarrow 0$. This suggests that the estimate gets increasingly accurate with better averaging, which is to be expected.

We can also use the standard method to relate the covariance of a function of random variables to the variances of the variables as follows [37]

$$\mathrm{Var}(\hat{\gamma}) = \mathrm{Var}\left(\frac{\hat{\lambda}_1}{\hat{\lambda}_2}\right) \approx \mathrm{Var}(\hat{\lambda}_1)\frac{1}{E^2(\hat{\lambda}_2)} + \mathrm{Var}(\hat{\lambda}_2)\frac{E^2(\hat{\lambda}_1)}{E^4(\hat{\lambda}_2)} \tag{4.24}$$

As an illustration consider the case when the signal space dimension is $d = 2$, and the signal power is equally distributed in both the dimensions. The lower bound on the SIR estimate can be numerically evaluated to be

$$\hat{\gamma} \geq \gamma + \gamma\left(\frac{2L^2 + \frac{10L}{\gamma} + \frac{12}{\gamma^2}}{(n-2)L^2 - \frac{4L}{\gamma}}\right) \tag{4.25}$$

Comparing (4.25) to (4.12) we notice that for the same γ the lower bound is tighter when the signal space dimension is 1. This can be understood by considering the fact that the smaller the signal space dimension, the more accurately can we get an estimate of the interference power by averaging over a larger number of eigenvalues. Consequently, we get a better estimate of the signal power which leads to a better estimate of the SIR.

Also, looking at (4.9) we note that we always tend to overestimate the SIR. This is due to the fact that we consider the interference covariance matrix to be diagonal and ignore the terms on the off-diagonals. This leads to an underestimation of the interference power, which leads to an overestimation of the SIR.

Chapter 5

Numerical Examples

In this chapter we numerically evaluate the performance of the SIR estimator and compare it to the analysis of the previous chapter. The SIR estimators are evaluated numerically in an hexagonal cellular system, using the following frame structure. The reverse traffic channel frame is 20ms long and operates at 9.6 Kbps. Therefore each frame consists of 192 bits and the frame rate is 50 frames/s. We employ a BPSK modulation scheme with transmitted symbols $a_i \in \{-1, 1\}$. The training sequence is assumed to be 25 bits long. The reason for the above choice of frame length and data rates is to emulate the specifications for an IS-95 system. However, we would like to point out that the choice of the training sequence is purely for illustration and does not conform to the IS-95 specifications.

For simulation purposes, we consider a Rayleigh fading channel with M=2 taps. The processing gain N and the number of interferers K assumed for the various simulations have been recorded in the titles of the figures. The noise floor is taken to be 20dB lower than the transmitted interference level. The Rayleigh distributed channel taps have been generated from normal random variables [17]. Suppose A and B are zero mean statistically independent Gaussian random variables, each having variance σ^2. If we define a new random variable R as $R = \sqrt{A^2 + B^2}$, then R is a Rayleigh distributed random variable with parameter σ^2. The performance of the estimator is evaluated using the mean, standard deviation and the absolute percentage error as measures. Note that the mean, standard deviation etc. have been plotted as a function of the number of frames observed for the estimation. As has been explained in chapter 3, we form a *moving average* or *Bartlett* estimate of the covariance matrix from the J most recent observation vectors. But we are interested in the *mean* value of the SIR estimate formed after observing J vectors. We observe one vector in every frame. For a fixed SIR, the power transmitted by each user and the channel taps remain the same in each trial. However, the noise samples and the information bits transmitted by the interferers is different in each trial. The *mean* is formed by averaging the SIR estimates formed from x independent trials. So, the value of n in equations (4.1) and (4.2) is Jx. In our simulations the value of x is assumed to be 100, unless otherwise stated in the title of the figure.

In Figure 5.1 we plot the SIR estimated by the ED and the PASTd estimators as a function of the number of frames over which averaging is done, for a fixed SIR of 9 dB. The plots are for a single trial. We note that both estimators perform quite well. The initial performance of the PASTd estimator depends to some extent on the initial values of the signal eigenvalues that we choose. Figure 5.2 depicts the value of $\hat{d}$, the estimated value of the signal subspace dimension. The true value of d here is 1. We note that the value of $\hat{d}$ increases initially, but goes to the value of 1 after sufficient averaging. Figure 5.3 shows the performance of the PASTd estimator for a very poor initial value. As can be seen, the estimator takes a very long time to converge to the actual SIR value. In Figure 5.4 we depict the mean of the 100 trials , one of which was plotted in Figure 5.1 as a function of the number of observed frames. Also plotted is the actual SIR and the lower bound on the mean as obtained from the analysis. The lower bound is so close to the actual SIR, that they appear to be the same graph. The reason for this is the large value of 100 that we have chosen for x in our simulations. The lower bound is highly sensitive to the value of $n = Jx$. The effect of a large x is essentially to average out the noise. However, our estimation procedure is sensitive largely to J, the number of observed frames. This is because while a large x averages out the noise, the interference is averaged out only when we average over a large number of observed frames. Hence for the estimator, the value of J dictates the performance.

For the same example in Figure 5.5 we plot the standard deviations of both the estimators and the lower bound obtained on the ED estimator from the analysis. We also plot the approximate expression for the standard deviation which was stated in Chapter 4. We see that standard deviation of the estimators improve (i.e., become lower) as the estimation time increases.

We plot the absolute percentage errors of the estimators as a function of the observed frames for the same example in Figure 5.6. We see that the percentage error of the ED estimator falls to below 20 percent after about 8 frames, and to below 10 percent after less than 15 frames.

Figure 5.7 depicts the percentage error of the SIR estimator for different values of the measured SIR as a function of the number of frames. We have plotted the error curves for SIR values of 4.6 dB, 6.2 dB and 9 dB. Despite the large variations in the SIR values, we note that the error curves are close to each other especially when the estimation is done after observing a larger number of frames. Thus for a given estimation time the estimator performance to within a given percentage of error is relatively insensitive to variations in the SIR.

Figure 5.8 depicts the mean SIR from the estimator and its lower bound as a function of the number of interferers, while keeping the signal power fixed. Also, the SIR has been estimated after an observation interval of 16 frames. In 5.9, we plot the absolute percentage error of the estimator for the example of Figure 5.8. We note that the percentage error increases slightly as the number of interferers increases, i.e as the SIR decreases. But for a decrease in SIR from 11dB to 1.8 dB, the increase in the percentage error is only from about 12 percent to 20 percent. Thus it is seen that the SIR estimate is reasonably close to the measured SIR with a slightly better accuracy at higher values of SIR (or lower number of interferers). This also emphasizes the fact that the estimator performs better at lower values of the load factor, $\frac{K}{N}$, than for higher values.

In Figure 5.10 we plot the estimator mean as a function of the number of frames observed for estimation for a measured SIR of 8.1 dB. Here, we have plotted the estimator means for the Processing gains of N=128 and N=256. As is expected, the mean obtained for the higher processing gain is closer to the lower bound. Also, the difference becomes more significant as the estimation time increases. Recall that the assumption of the interference covariance matrix being diagonal is more valid for larger N. In Figure 5.11 we depict the absolute percentage error for the example of Figure 5.10. We see that for N=256, the error falls to below 20 percent after 7 frames and to below 10 percent after 11 frames. Thus we have a significant improvement in the performance for a larger processing gain as the estimation time increases.

In Figure 5.12 we plot the error performance of the ED estimator as a functions of the observed number of frames for different values of SIR. Here we have taken K, the number of interferers to be 20. We note that the error curves resemble those error curves of 5.7. The curves are quite close to each other despite the large variations in SIR. In Figure 5.13 the noise power levels have been varied to study the effect of the noise variance on the estimator performance. Once again, the absolute percentage errors have been plotted as a function of the number of observed frames. We observe that as the noise level is taken to be lower, the performance improves. This is only to be expected since, lowering the noise power leads to an increase in the SIR for the same channel conditions. If the noise is lower, inaccuracies in its estimation affect the performance of the estimator to a smaller degree than if it was higher.

In Figure 5.14 we attempt to parameterize the performance of the estimators in terms of the velocity of the mobiles. The starting position of the mobile receiver is uniformly distributed over the cell area. The mobile moves with a constant speed in a direction uniformly distributed in $[0, 2\pi]$. In addition to the raleigh fading factor we also consider a shadow fading factor $s(t)$ assumed to be log-normally distributed with a mean of 0 dB, and a log-standard deviation of $\sigma_f = 8$ dB. The shadow fading is further assumed to have to have the time correlation function proposed in [36], which has been derived based on field experimental data. If

$z(t) = (10/\sigma_f) \log_{10} s(t)$, then

$$E[z(t+\tau)z(t)] = e^{-v\tau/X} \ , \tag{5.1}$$

where v is the velocity of the mobile user. The parameter X is the effective correlation distance of the shadow fading, and is assumed to be 43 m. We have plotted the percentage error graphs for widely varying mobile velocities. We note that the error curves for all the cases depicted are close to each other proving that the estimator is quite robust to mobile velocities.

In Figure 5.15, we depict the SIR tracking abilities of both the estimators in the context of a constantly time varying SIR. Here the length of the sliding window for the ED estimator J is 20. The value of the forgetting factor β for the PASTd estimator is taken to be 0.7. The SIR is plotted as function of time for more clarity. For this example the SIR variations are quite large. These variations have been achieved by adjusting the power of user 0. Note that the variations can also be achieved by adjusting the interference power. In the practical case of a large number of interferers, on account of the small cross correlation between them, a significant change in the interference power is obtained only if a large number of interferers change their powers significantly. Here the SIR varies every 0.8 sec or equivalently every 40 frames. We note that both the estimators track the SIR quite well, with the PASTd estimator outperforming the ED estimator slightly. Plotted in 5.16 is the variation of $\hat{d}$, the estimated value of the signal subspace dimension as a function of time. We note that when the SIR changes, $\hat{d}$ tends to increase, and then drops down to the true value of 1 after sufficient averaging.

In Figure 5.17 we plot the SIR tracking of the estimators for a more rapidly varying SIR again with large SIR variations. The SIR here changes every 0.4 sec, or equivalently every 20 frames. In Figure 5.18 also we plot a sample path for the estimators for the same SIR variation as the previous figure but with a different initialization for the PASTd estimator. We note that the estimators depict peaks at the points where the SIR changes, but they adapt quite quickly to the changed environment.

In Figure 5.19 we plot the mean performances of the estimators averaged over 10 trials for the slowly varying SIR of Figure 5.15. In Figure 5.20 the estimator means averaged over 10 trials are plotted for the more rapidly varying SIR of Figures 5.17 and 5.18.

We note that as the SIR variation becomes more rapid, the performance of both the estimators deteriorate. This is to be expected because the estimators need some time to adapt to the changed SIR and converge to the new value. If the SIR changes before they start converging, they are unable to track the changes effectively. We note that at the transitions points of the SIR, the PASTd estimator in particular exhibits sharp peaks, but it adapts quite quickly after that.

In Figure 5.21 we depict the tracking abilities of the estimators for the case of subtle variations in the SIR. We note that the estimators keep fairly good track of the SIR. We plot the percentage error graphs for the example of Figure 5.22 in Figure 5.21. We note that the errors are very small for both the estimators. Thus the estimators perform very well in the context of a very gently varying SIR.

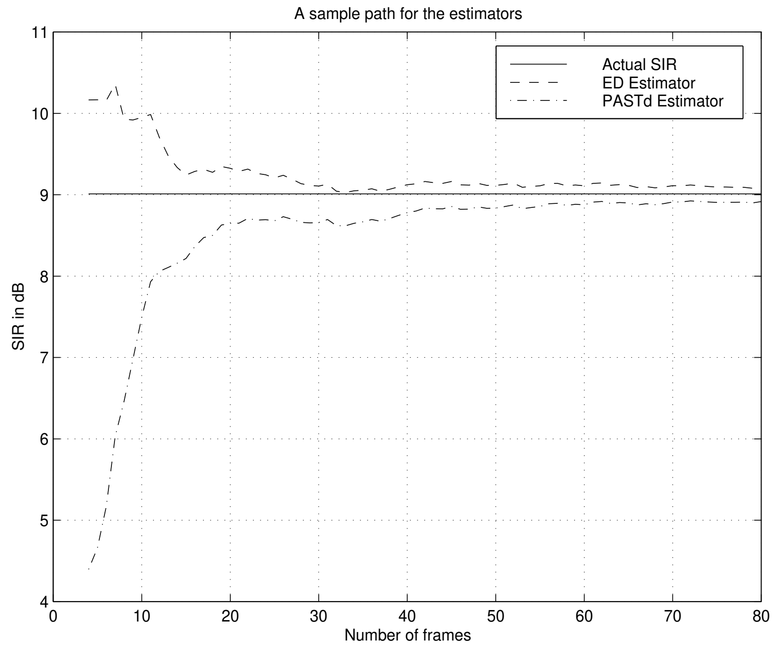

Figure 5.1: SIR estimate of the two estimators vs. number of frames observed - single trial

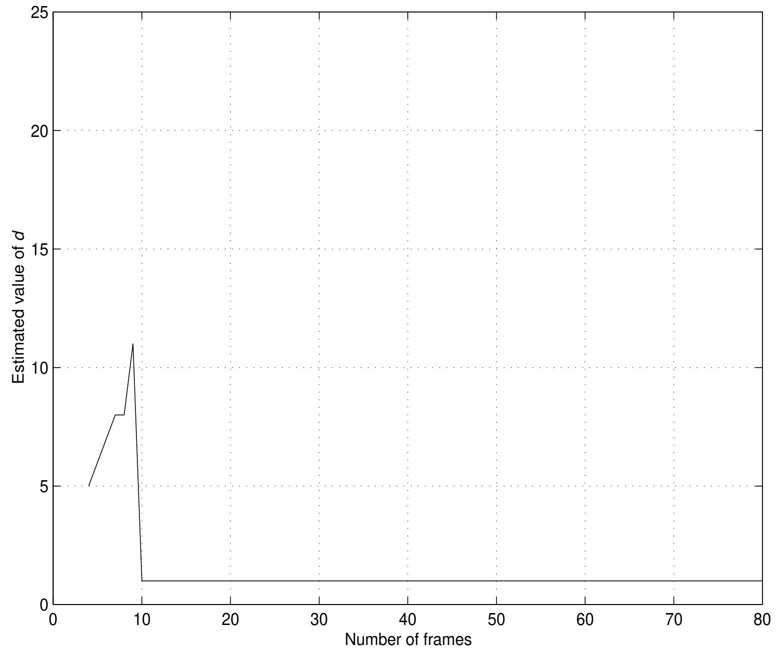

Figure 5.2: Value of $\hat{d}$ - the estimated signal subspace dimension vs. number of frames observed

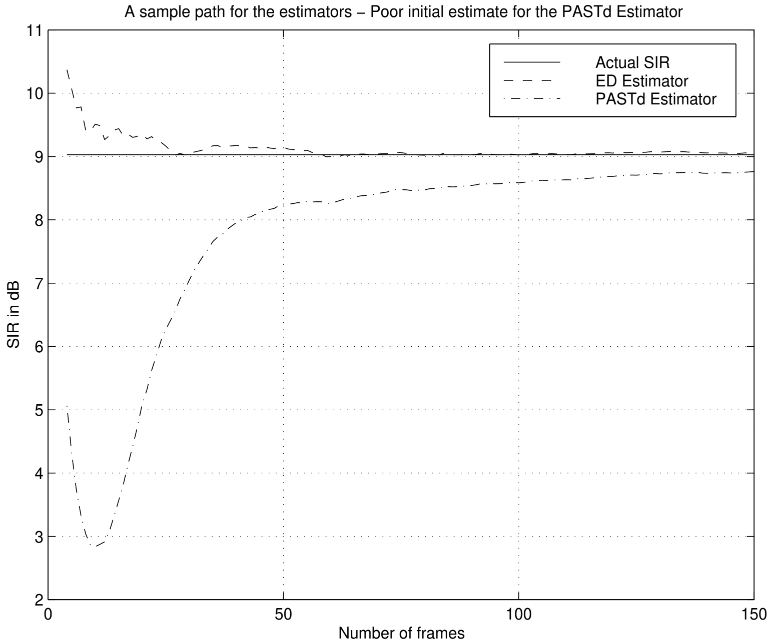

Figure 5.3: SIR estimate of the two estimators vs. number of frames observed - single trial

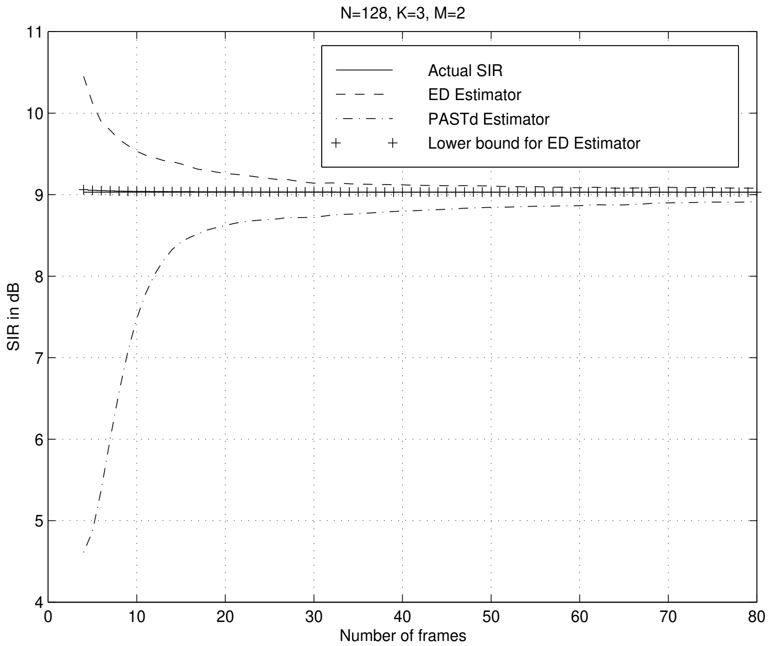

Figure 5.4: Mean SIR of the estimators and the analytical lower bound of the ED estimator vs. number of frames observed

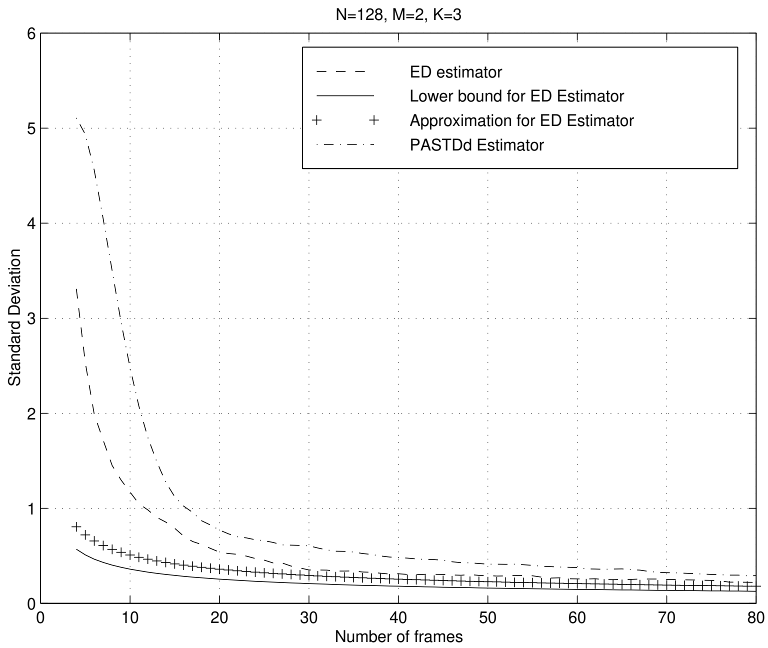

Figure 5.5: Standard Deviation of the estimators and the analytical lower bound of the ED estimator vs. number of frames observed

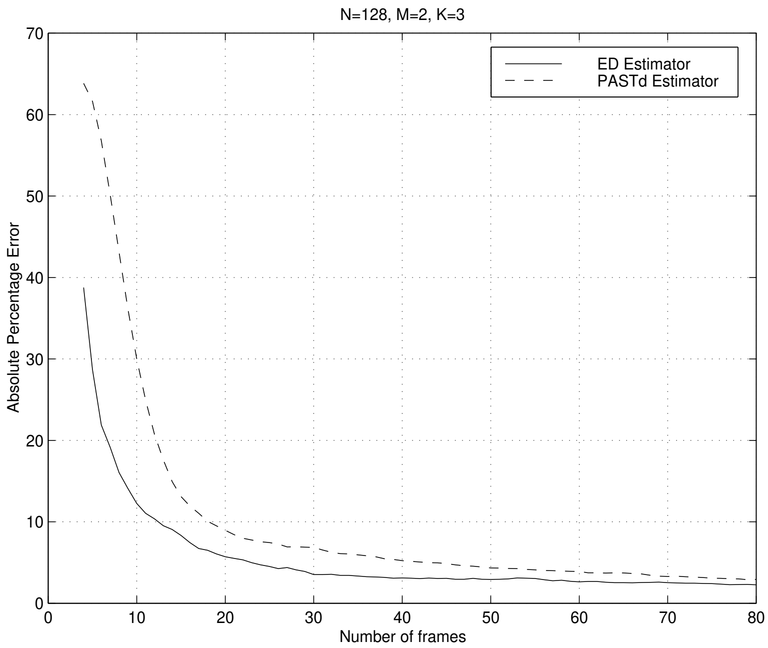

Figure 5.6: Percentage error of the estimators vs. number of observed frames

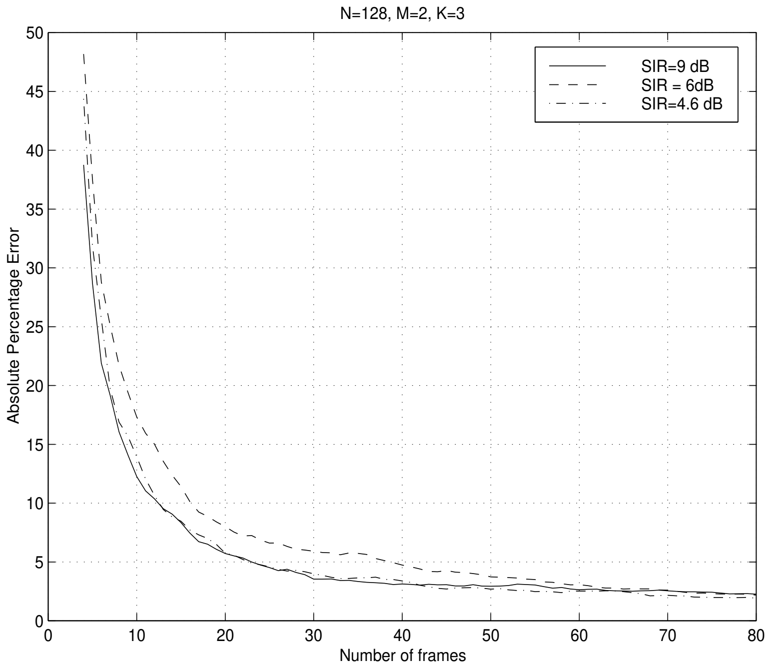

Figure 5.7: Percentage error of the ED estimator vs. number of observed frames for different values of the SIR

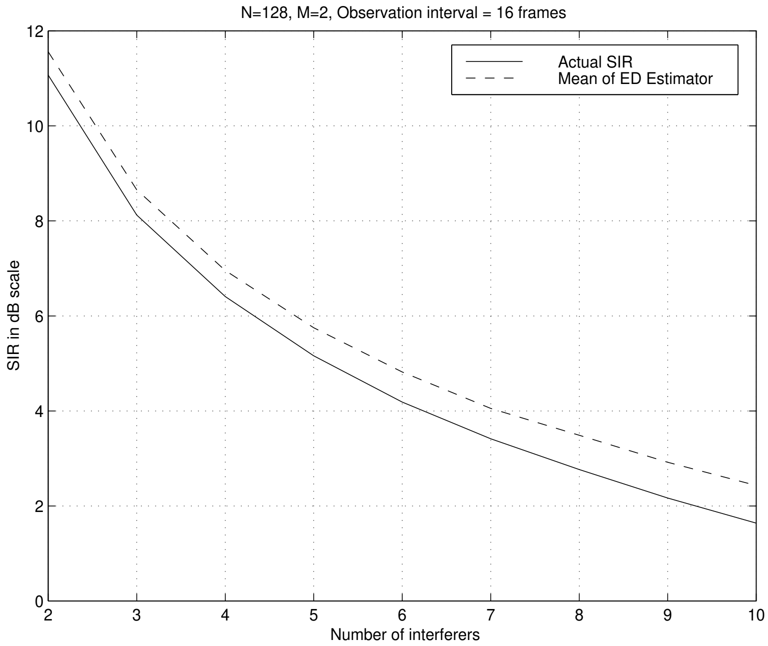

Figure 5.8: Actual SIR and ED estimator mean as a function of the number of interferers

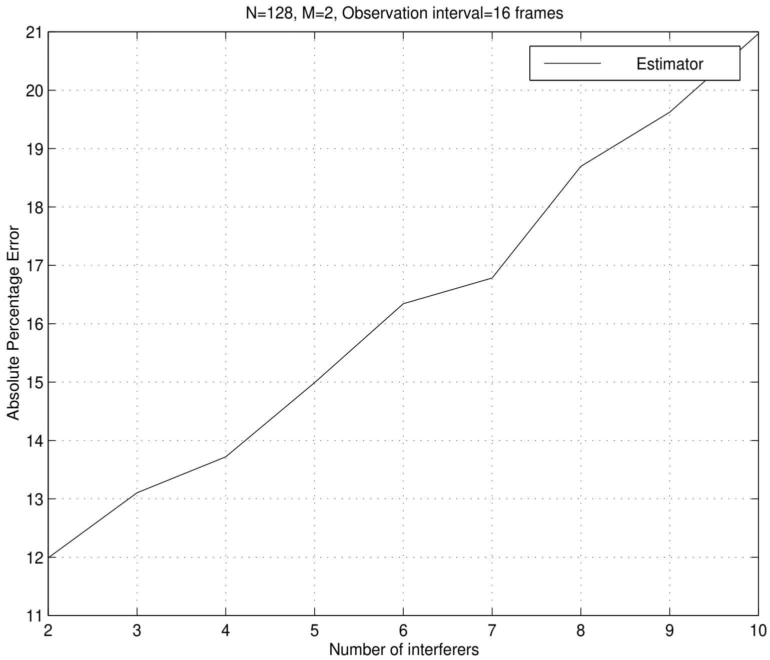

Figure 5.9: Percentage error of ED estimator as a function of the number of interferers

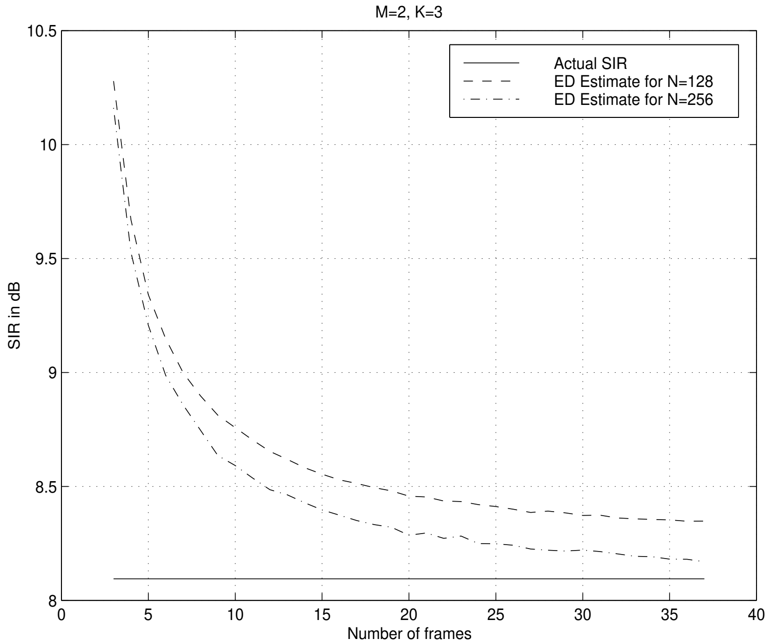

Figure 5.10: Mean of the ED estimator for different processing gains as a function of the number of observed frames

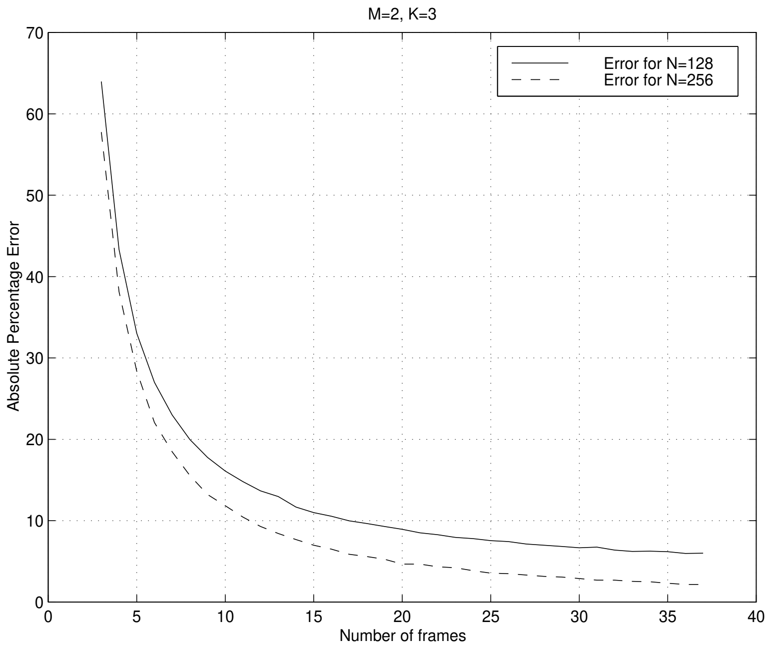

Figure 5.11: Absolute percentage error of the ED estimator for different processing gains as a function of the number of observed frames

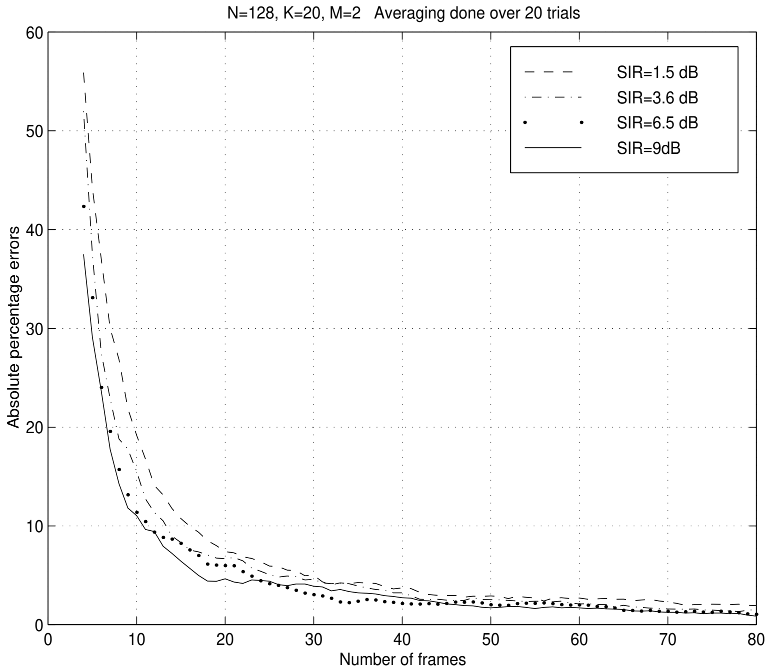

Figure 5.12: Percentage error of the ED estimator vs. number of observed frames for different values of the SIR for 20 interferers

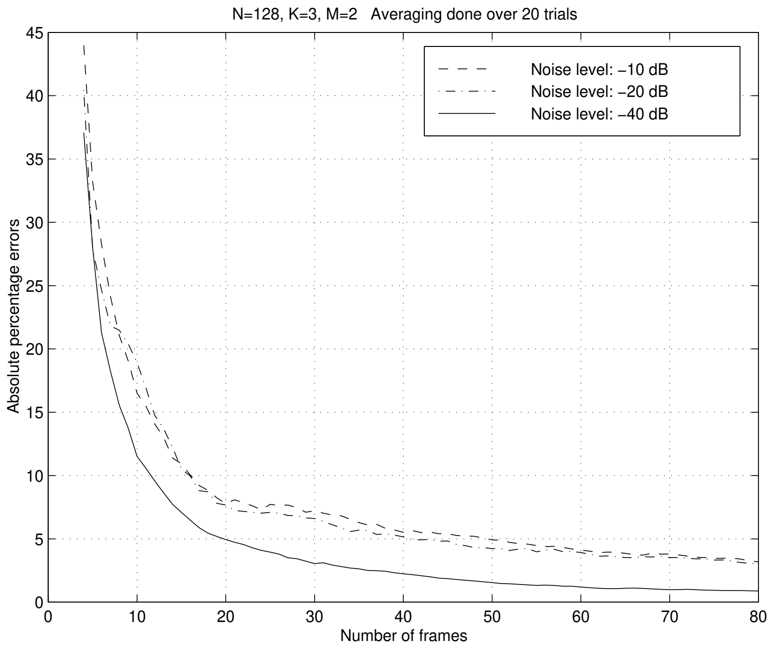

Figure 5.13: Percentage error of the ED estimator vs. number of observed frames for different noise powers

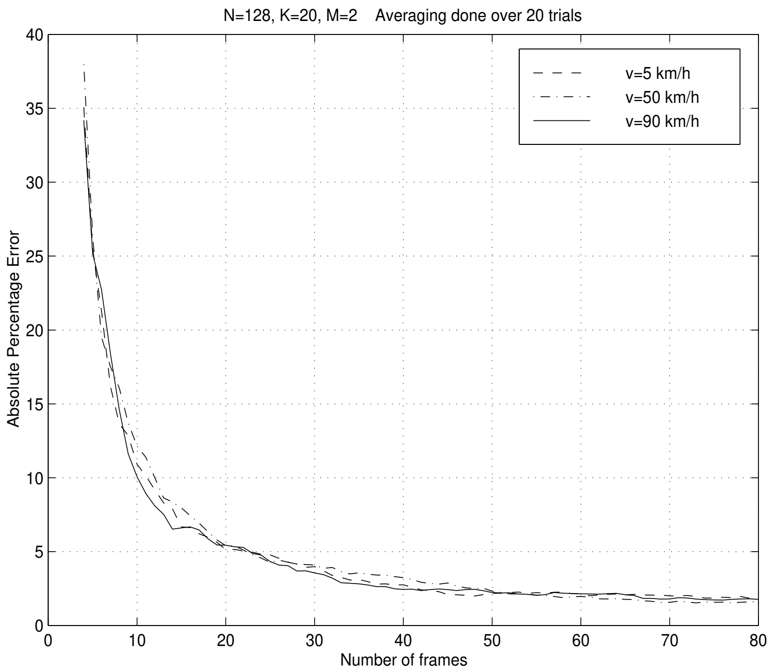

Figure 5.14: Percentage error of the ED estimator vs. number of observed frames for different mobile velocities

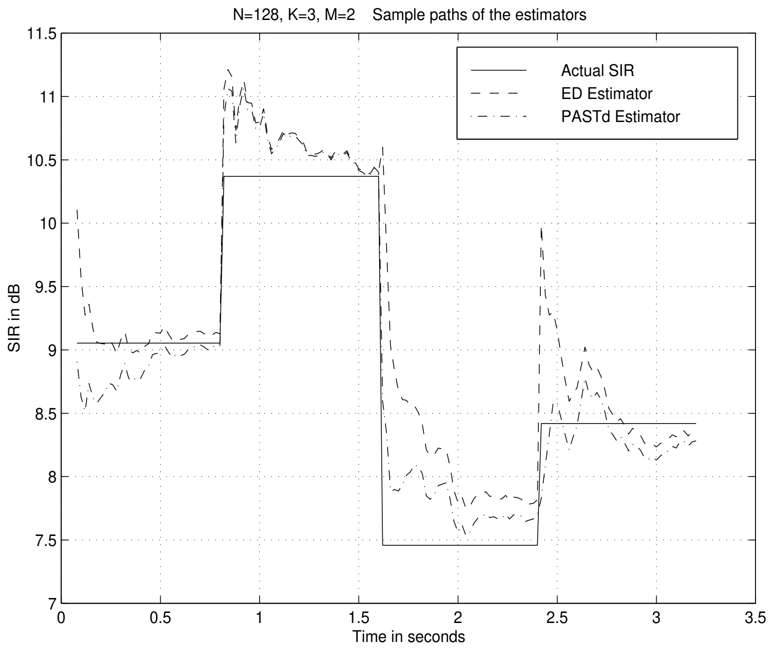

Figure 5.15: Tracking ability of the estimators for a time varying SIR

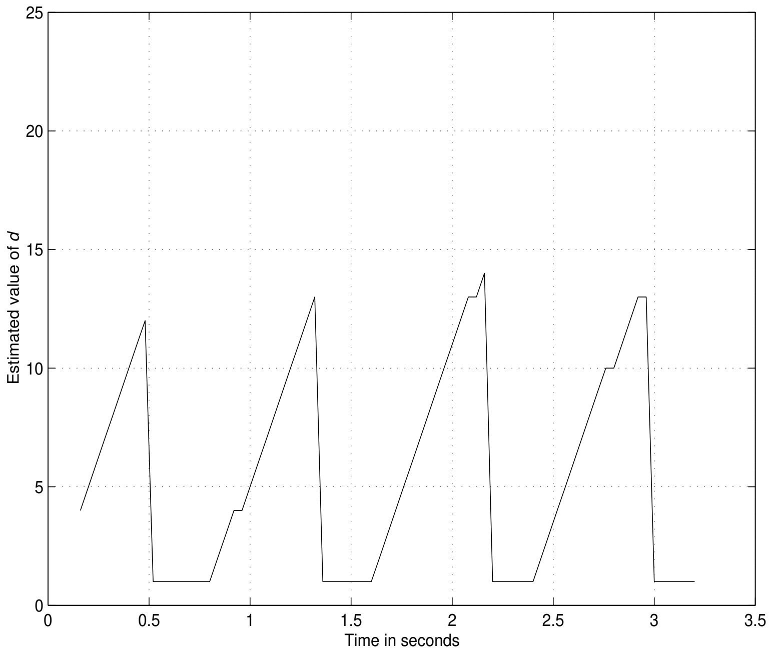

Figure 5.16: Value of $\hat{d}$ - the estimated signal subspace dimension vs. number of frames observed

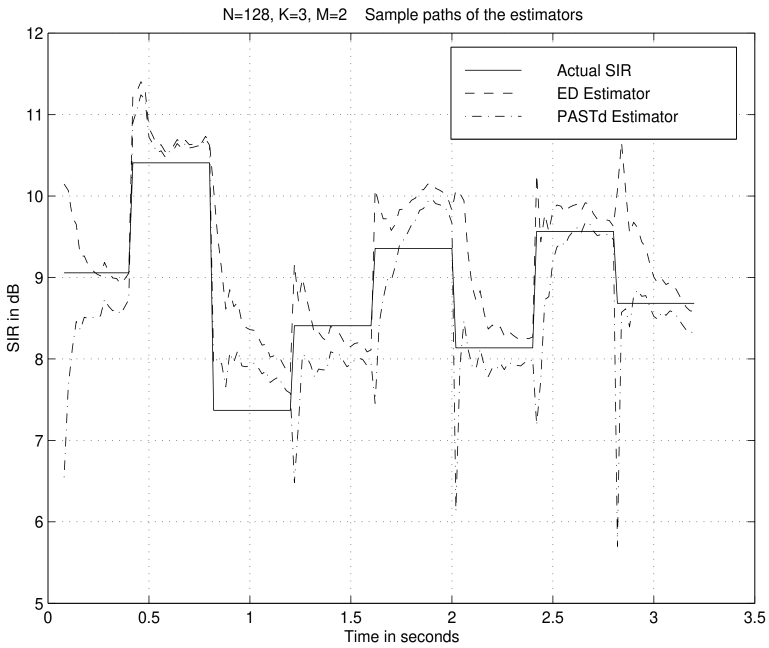

Figure 5.17: Tracking ability of the estimators for a more rapidly time varying SIR

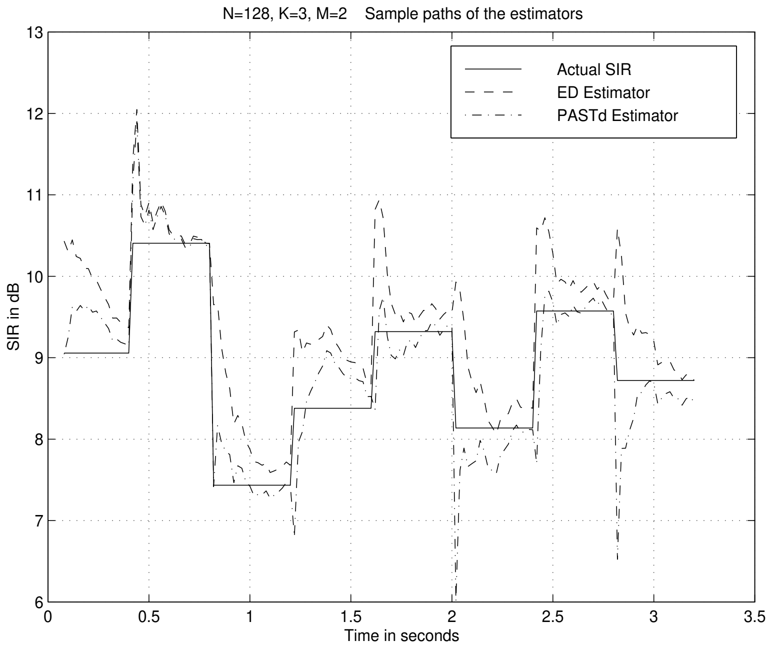

Figure 5.18: Tracking ability of the estimators for a more rapidly time varying SIR with a different initialization for the PASTd estimator

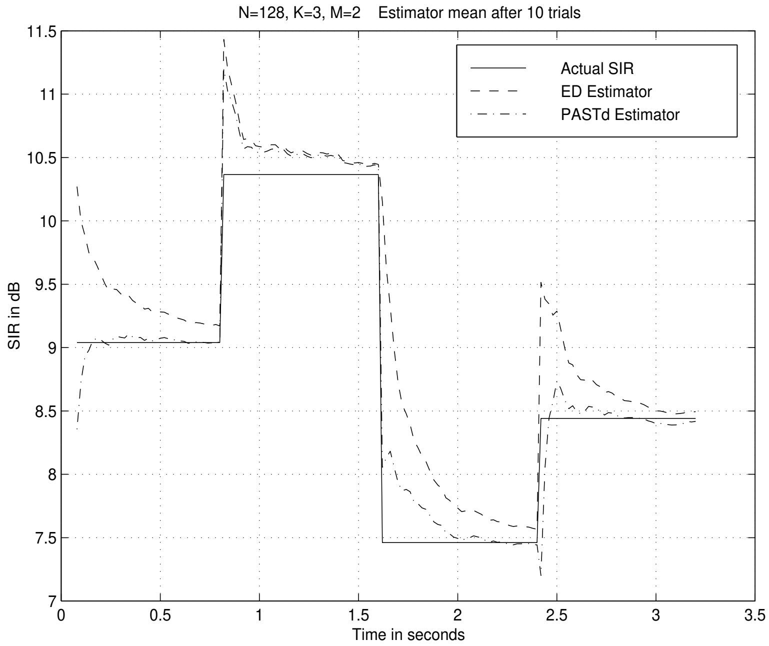

Figure 5.19: Mean performance of the estimators for the less rapidly varying SIR

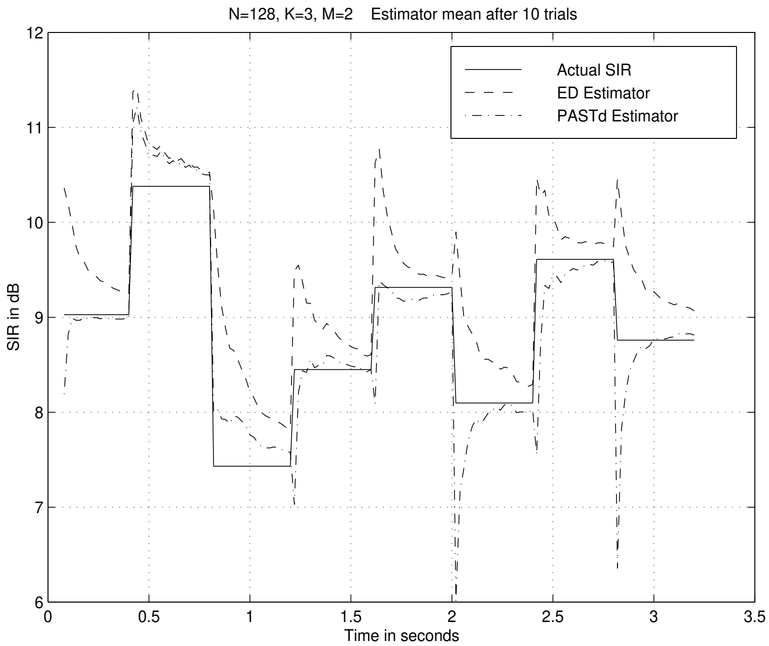

Figure 5.20: Mean performance of the estimators for the more rapidly varying SIR

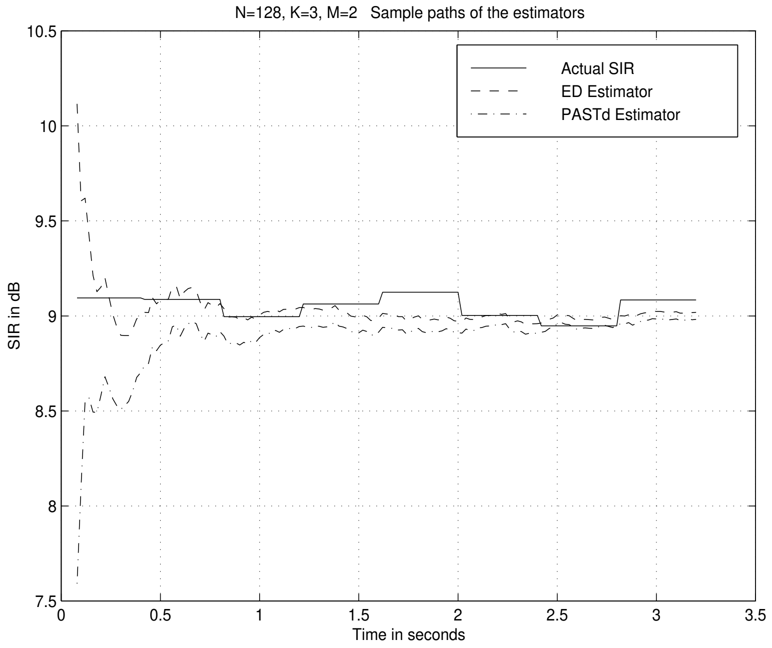

Figure 5.21: Tracking ability of the estimators for small SIR variations

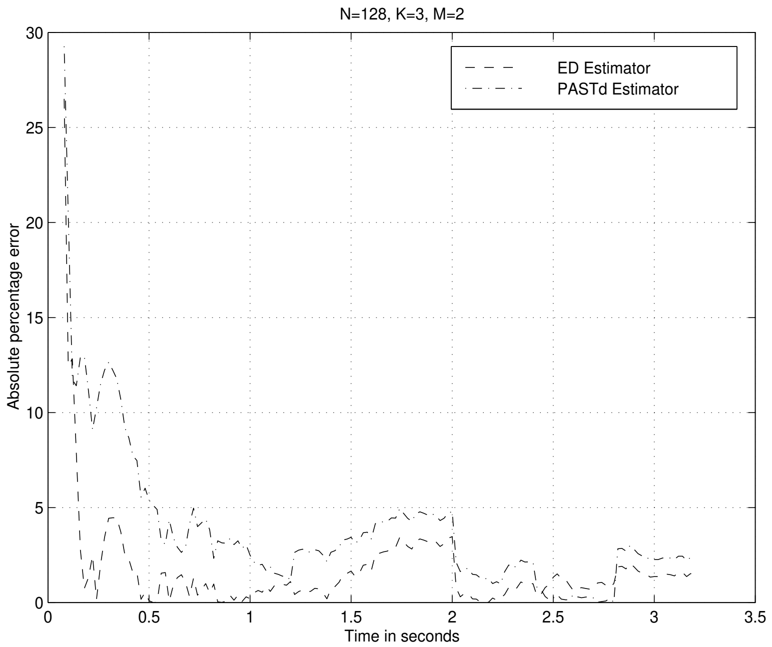

Figure 5.22: Error performance of the estimators for small SIR variations

Chapter 6

Conclusions

In this thesis we have studied the practical problem of obtaining accurate real time measurements of the SIR for CDMA cellular systems. We have derived a subspace based estimation method, that is based on an eigenvector decomposition of the sample covariance matrix of the received signal. We have also looked at a less complex subspace tracking algorithm.

We have shown via analytical bounds and numerical examples that the ED based SIR estimator is able to estimate the true SIR within an error of 10 percent after an observation interval of only about 11 frames for a processing gain of 256 and an observation interval of less than 15 frames for a processing gain of 128. The subspace method was shown to be relatively insensitive to the actual SIR values. The SIR tracking abilities of the ED estimator and the PASTd estimator have been illustrated via examples. It is seen that they are both able to track variations in the SIR reasonably well with the PASTd estimator performing slightly better than the ED estimator, especially with good initialization. One approach could be to use the ED estimator to obtain an estimate of the signal space dimension as well as estimates of the covariance matrix eigenvalues with which to initialize the PASTd estimator after which the PASTd estimator could be made to track the SIR. We believe that the above approach for SIR estimation can be used in power control and handoff algorithms. This method did not require any prior information about the channel. Another attractive feature of the subspace based technique is that it allows easy integration into the multiuser architectures like the MMSE and the decorrelator [30] which are essentially based on projecting the received signal onto a subspace orthogonal to that of the interference (plus noise) subspace. Yet another feature that makes the proposed SIR estimation technique desirable is that it allows for easy implementation on existing VLSI hardware and DSP devices. Also as this technique does not require knowledge about the code sequences of the various users, we believe that it can be used for SIR estimation on the forward link as well as the reverse link.

Appendix A

Derivation of $\boldsymbol{R}_I$

The matrix $\boldsymbol{R}_I$ from (2.17) can be simplified as

$$\begin{aligned}\boldsymbol{R}_I &= E[\sum_{j=1}^{K}(\boldsymbol{a}_j^l\boldsymbol{r}_{j0}^l+\boldsymbol{a}_j^r\boldsymbol{r}_{j0}^r)\boldsymbol{h}_{j0}\sum_{i=1}^{K}\boldsymbol{h}_{i0}^H(\boldsymbol{r}_{i0}^{lH}\boldsymbol{a}_i^{lH}+\boldsymbol{r}_{i0}^{rH}\boldsymbol{a}_i^{rH})] \\ &= \boldsymbol{R}_I^{ll}+\boldsymbol{R}_I^{lr}+\boldsymbol{R}_I^{rl}+\boldsymbol{R}_I^{rr} \qquad \text{(A.1)}\end{aligned}$$

where

$$\boldsymbol{R}_I^{ll} = E[\sum_{j=1}^{K}\boldsymbol{a}_j^l\boldsymbol{r}_{j0}^l\boldsymbol{h}_{j0}\boldsymbol{h}_{j0}^H\boldsymbol{r}_{j0}^{lH}\boldsymbol{a}_j^{lH}] \qquad \text{(A.2)}$$

$$\boldsymbol{R}_I^{lr} = E[\sum_{j=1}^{K}\boldsymbol{a}_j^l\boldsymbol{r}_{j0}^l\boldsymbol{h}_{j0}\boldsymbol{h}_{j0}^H\boldsymbol{r}_{j0}^{rH}\boldsymbol{a}_j^{rH}] \qquad \text{(A.3)}$$

$$\boldsymbol{R}_I^{rl} = E[\sum_{j=1}^{K}\boldsymbol{a}_j^r\boldsymbol{r}_{j0}^r\boldsymbol{h}_{j0}\boldsymbol{h}_{j0}^H\boldsymbol{r}_{j0}^{lH}\boldsymbol{a}_j^{lH}] \qquad \text{(A.4)}$$

$$\boldsymbol{R}_I^{rr} = E[\sum_{j=1}^{K}\boldsymbol{a}_j^r\boldsymbol{r}_{j0}^r\boldsymbol{h}_{j0}\boldsymbol{h}_{j0}^H\boldsymbol{r}_{j0}^{rH}\boldsymbol{a}_j^{rH}] \qquad \text{(A.5)}$$

Recall that $\boldsymbol{a}$ is an $L \times 1$ column vector, $\boldsymbol{r}$ is a $1 \times M$ row vector and $\boldsymbol{h}$ is a $M \times 1$ column vector. We can expand the terms on the RHS of the above equations in terms of matrices $\boldsymbol{I}$, $\boldsymbol{U}$ and $\boldsymbol{L}$ where $\boldsymbol{I}$ is the identity matrix and $\boldsymbol{L} = \boldsymbol{U}^T$ is given as

$$\boldsymbol{L} = \begin{pmatrix} 0 & 0 & .... & 0 \\ 1 & 0 & .... & 0 \\ 0 & 1 & .... & 0 \\ 0 & .. & 1 & 0 \end{pmatrix} \qquad \text{(A.6)}$$

It follows that we can write

$$\boldsymbol{R}_I^{ll} = E[\sum_{j=1}^{K}\boldsymbol{r}_{j0}^l\boldsymbol{h}_{j0}\boldsymbol{h}_{j0}^H\boldsymbol{r}_{j0}^{lH}]\boldsymbol{I} \qquad \text{(A.7)}$$

$$\boldsymbol{R}_I^{lr} = E[\sum_{j=1}^{K} \boldsymbol{r}_{j0}^{l} \boldsymbol{h}_{j0} \boldsymbol{h}_{j0}^{H} \boldsymbol{r}_{j0}^{rH}] \boldsymbol{L} \tag{A.8}$$

$$\boldsymbol{R}_I^{rl} = E[\sum_{j=1}^{K} \boldsymbol{r}_{j0}^{r} \boldsymbol{h}_{j0} \boldsymbol{h}_{j0}^{H} \boldsymbol{r}_{j0}^{lH}] \boldsymbol{U} \tag{A.9}$$

$$\boldsymbol{R}_I^{rr} = E[\sum_{j=1}^{K} \boldsymbol{r}_{j0}^{r} \boldsymbol{h}_{j0} \boldsymbol{h}_{j0}^{H} \boldsymbol{r}_{j0}^{rH}] \boldsymbol{I} \tag{A.10}$$

By virtue of the assumptions about the channel taps of the various users being uncorrelated, we can write

$$E[\sum_{j=1}^{K} \boldsymbol{r}_{j0}^{l} \boldsymbol{h}_{j0} \boldsymbol{h}_{j0}^{H} \boldsymbol{r}_{j0}^{lH}] = \sum_{j=1}^{K} \sum_{p=1}^{M} E[(r_{j0p}^{l})^2] \cdot E[h_{j0p} h_{j0p}^{H}] \tag{A.11}$$

$$E[\sum_{j=1}^{K} \boldsymbol{r}_{j0}^{l} \boldsymbol{h}_{j0} \boldsymbol{h}_{j0}^{H} \boldsymbol{r}_{j0}^{rH}] = \sum_{j=1}^{K} \sum_{p=1}^{M} E[r_{j0p}^{l} r_{j0p}^{r}] \cdot E[h_{j0p} h_{j0p}^{H}] \tag{A.12}$$

$$E[\sum_{j=1}^{K} \boldsymbol{r}_{j0}^{r} \boldsymbol{h}_{j0} \boldsymbol{h}_{j0}^{H} \boldsymbol{r}_{j0}^{lH}] = \sum_{j=1}^{K} \sum_{p=1}^{M} E[r_{j0p}^{r} r_{j0p}^{l}] \cdot E[h_{j0p} h_{j0p}^{H}] \tag{A.13}$$

$$E[\sum_{j=1}^{K} \boldsymbol{r}_{j0}^{r} \boldsymbol{h}_{j0} \boldsymbol{h}_{j0}^{H} \boldsymbol{r}_{j0}^{rH}] = \sum_{j=1}^{K} \sum_{p=1}^{M} E[(r_{j0p}^{r})^2] \cdot E[h_{j0p} h_{j0p}^{H}] \tag{A.14}$$

Thus $\boldsymbol{R}_I$ is in the form of a symmetric tridiagonal matrix, i.e. the only non-zero terms in the matrix are the ones on the diagonal and the two off-diagonals. The matrix $\boldsymbol{R}_I$ can be written as

$$\boldsymbol{R}_I = \begin{pmatrix} \alpha & \beta & 0 & \cdots & 0 \\ \beta & \alpha & \beta & \cdots & 0 \\ 0 & \beta & \alpha & \ddots & \\ \vdots & & \ddots & \ddots & \beta \\ 0 & \cdots & \cdots & \beta & \alpha \end{pmatrix}, \tag{A.15}$$

where

$$\alpha = \sum_{j=1}^{K} \sum_{p=1}^{M} E[(r_{j0p}^{r})^2 + (r_{j0p}^{l})^2] \cdot E[h_{j0p} h_{j0p}^{H}] \tag{A.16}$$

$$\beta = \sum_{j=1}^{K} \sum_{p=1}^{M} E[r_{j0p}^{r} r_{j0p}^{l}] \cdot E[h_{j0p} h_{j0p}^{H}] \tag{A.17}$$

We attempt to simplify the terms in the above interference covariance matrix. Consider the correlation terms, r_{j0p}^{l} and r_{j0p}^{r}:

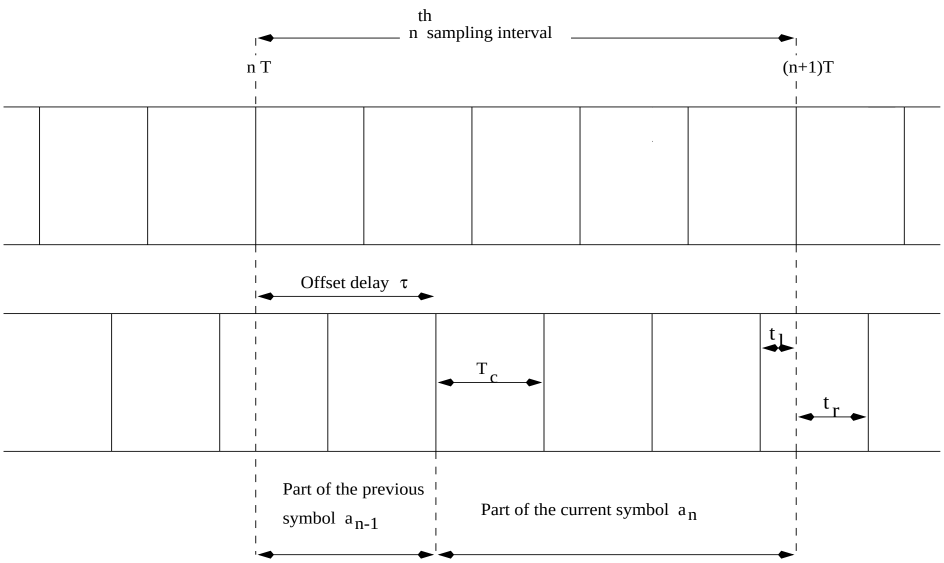

Figure A.1: Illustrative example with N=5, and m=4

In any sampling interval nT to $(n+1)T$, we have a part of the present symbol $a_{j,n}$ for every user j, and a part of the previous symbol $a_{j,n-1}$.

Suppose, for the j^{th} user, in the p^{th} multipath, we have $(m-1)$ complete chips and part of the m^{th} chip of a_n in the given interval. Then,

$$T - \tau_{j0p} = (m-1)T_c + t_l \tag{A.18}$$

Here, t_l is that part of the m^{th} chip which is in the n^{th} interval. So, $t_r = T_c - t_l$ is the part of the chip which will fall in the next interval. Similarly, in the given interval we will have a part of the m^{th} chip and $(N-m)$ complete chips of the previous symbol. Then, r^l_{j0p} can be written as

$$r^l_{j0p} \cdot T = \sum_{i=1}^{N-m} c_0[i](c_j[m+i-1]t_r + c_j[m+i]t_l) + c_0[N-m+1]c_j[N]t_r \tag{A.19}$$

Similarly, r^r_{j0p} can be written as

$$r^r_{j0p} \cdot T = c_0[N-m+1]c_j[1]t_l + \sum_{i=N-m+2}^{N} c_0[i](c_j[m+i-1-N]t_r + c_j[m+i-N]t_l) \tag{A.20}$$

Note that, the RHS of the above equations need to be divided by $T = NT_c$ in order to normalize the correlation terms. The code sequence of the desired user is either known or deterministic, while those of the other users are pseudorandom sequences. Hence

$$E[c_j[k]] = 0 \qquad \forall k, \forall j = 1, 2, ...K. \tag{A.21}$$

Also, since the chips are independent of each other

$$E[c_j[i]c_j[p]] = 0 \qquad \forall i \neq p \tag{A.22}$$

The above conditions lead to

$$\begin{aligned} T^2 E[r^l_{j0p} r^r_{j0p}] &= E[(c_j[m])^2 c_0[1] t_r c_0[N] t_l] \\ &= c_0[1] c_0[N] E[t_r t_l] \end{aligned} \tag{A.23}$$

Recall that we had modeled the multipath delays τ_{j0p}'s as uniform random variables $\in [0, T]$. It follows that t_r and t_l are uniform random variables $\in [0, T_c]$. Since $t_r = T_c - t_l$, we can write

$$\begin{aligned} E[t_r t_l] &= E[t_r(T_c - t_r)] \\ &= T_c E[t_r] - E[(t_r)^2] \\ &= T_c(T_c/2) - (T_c^2/3) \\ &= T_c^2/6 \end{aligned} \tag{A.24}$$

Hence

$$E[r^l_{j0p} r^r_{j0p}] = c_0[1] c_0[N] \frac{T_c^2}{6T^2} = c_0[1] c_0[N] \frac{1}{6N^2} \tag{A.25}$$

The above equation is true $\forall p, j$.

Since

$$[(r^l_{j0p})^2 + (r^r_{j0p})^2] = (r^l_{j0p} + r^r_{j0p})^2 - 2(r^l_{j0p} r^r_{j0p}) \tag{A.26}$$

we can write

$$E[(r^l_{j0p})^2 + (r^r_{j0p})^2] = E[(r^l_{j0p} + r^r_{j0p})^2] - 2E[r^l_{j0p} r^r_{j0p}] \tag{A.27}$$

Adding (A.19) and (A.20) we get

$$\begin{aligned} (r^l_{j0p} + r^r_{j0p}) \cdot T &= \sum_{i=1}^{N-m} c_0[i](c_j[m+i-1]t_r + c_j[m+i]t_l) \\ &+ c_0[N-m+1](c_j[N]t_r + c_j[1]t_l) \\ &+ \sum_{i=N-m+2}^{N} c_0[i](c_j[m+i-1-N]t_r + c_j[m+i-N]t_l) \end{aligned} \tag{A.28}$$

By rearranging the terms, the above equation can be written as

$$\begin{aligned}(r^l_{j0p} + r^r_{j0p}) \cdot T &= \sum_{i=1}^{m-1} c_j[i](c_0[N+i-m]t_l + c_0[N+i-m+1]t_r) \\ &+ c_j[m](c_0[N]t_l + c_0[1]t_r) \\ &+ \sum_{i=m+1}^{N} c_j[i](c_0[i-m]t_l + c_0[i-m+1]t_r) \qquad \text{(A.29)}\end{aligned}$$

Now squaring the above equation and taking expectation of both sides, we get

$$\begin{aligned}E[(r^l_{j0p} + r^r_{j0p})^2] \cdot T^2 &= \sum_{i=1}^{m-1} E(t_l^2 + t_r^2 + 2c_0[N+i-m]c_0[N+i-m+1]t_r t_l) \\ &+ E(t_l^2 + t_r^2 + 2c_0[N]c_0[1]t_r t_l) \\ &+ \sum_{i=m+1}^{N} E(t_l^2 + t_r^2 + 2c_0[i-m]c_0[i-m+1]t_r t_l) \qquad \text{(A.30)}\end{aligned}$$

$$\begin{aligned}&= NE[t_l^2 + t_r^2] + 2c_0[1]c_0[N]E[t_r t_l] \\ &+ 2\sum_{k=1}^{N-1} c_0[k]c_0[k+1]E[t_r t_l] \qquad \text{(A.31)}\end{aligned}$$

As we have seen before

$$T^2 E[r^l_{j0p} r^l_{j0p}] = c_0[1]c_0[N]E[t_r t_l] \qquad \text{(A.32)}$$

Therefore

$$E[(r^l_{j0p})^2 + (r^r_{j0p})^2] \cdot T^2 = NE[t_r^2 + t_l^2] + 2E[t_r t_l]\sum_{k=1}^{N-1} c_0[k]c_0[k+1] \qquad \text{(A.33)}$$

Now

$$\begin{aligned}E[t_r^2 + t_l^2] &= E[t_r^2 + (T_c - t_r)^2] \\ &= 2E[t_r^2] - 2T_c E[t_r] + T_c^2 \\ &= 2T_c^2/3 - 2T_c \cdot T_c/2 + T_c^2 \\ &= 2T_c^2/3 \qquad \text{(A.34)}\end{aligned}$$

So finally we get

$$E[(r^l_{j0p})^2 + (r^r_{j0p})^2] = \frac{2}{3N} + \frac{1}{3N^2}\sum_{k=1}^{N-1} c_0[k]c_0[k+1] \qquad \text{(A.35)}$$

Returning to the $\boldsymbol{R}_I$ matrix and denoting $E[h_{j0p}h_{j0p}^H] = \sigma^2_{h_{j0p}}$, the terms in $\boldsymbol{R}_I$ can be written as

$$\alpha = (\sum_{j=1}^{K}\sum_{p=1}^{M}\sigma^2_{j0p})\left(\frac{2}{3N} + \frac{1}{3N^2}\sum_{k=1}^{N-1} c_0[k]c_0[k+1]\right) \tag{A.36}$$

$$\beta = (\sum_{j=1}^{K}\sum_{p=1}^{M}\sigma^2_{j0p})\left(\frac{1}{6N^2}c_0[1]c_0[N]\right) \tag{A.37}$$

Appendix B

The Multivariate Normal Distribution

B.1 Definition and properties

The *mean* or *expectation* of a random $m \times 1$ vector $\boldsymbol{X} = (X_1 \ \ldots \ X_m)^{'}$ is defined to be the vector of expectations:

$$E(\boldsymbol{X}) = \begin{pmatrix} E(X_1) \\ . \\ . \\ . \\ E(X_m) \end{pmatrix} \tag{B.1}$$

If $\boldsymbol{X}$ has mean $\boldsymbol{\mu}$, the covariance matrix $\boldsymbol{X}$ is defined to be the $m \times m$ matrix

$$\Sigma \equiv \mathrm{Cov}(\boldsymbol{X}) = E[(\boldsymbol{X} - \boldsymbol{\mu})(\boldsymbol{X} - \boldsymbol{\mu})^{'}] \tag{B.2}$$

The $i - j$th element of Σ is

$$\sigma_{ij} = E[(X_i - \mu_i)(X_j - \mu_j)], \tag{B.3}$$

the covariance between X_i and X_j, and the $i - i$th element is

$$\sigma_{ii} = E[(X_i - \mu_i)^2], \tag{B.4}$$

the variance of X_i, so that the diagonal elements of Σ must be nonnegative. The class of covariance matrices coincides with the class of *non-negative definite* matrices. Recall that an $m \times m$ symmetric matrix A is called non-negative definite if

$$\boldsymbol{\alpha} A \boldsymbol{\alpha} \geq 0, \qquad \forall \ \boldsymbol{\alpha} \in R^m \tag{B.5}$$

B.2 Normal Distributions

The $m \times 1$ random vector $\boldsymbol{X}$ is said to have an $m-$variate normal distribution if, for every $\boldsymbol{\alpha} \in R^m$, the distribution of $\boldsymbol{\alpha}'\boldsymbol{X}$ is univariate normal. If $\boldsymbol{X}$ has an $m-$variate normal distribution, then both $\boldsymbol{\mu} \equiv E(\boldsymbol{X})$ and $\boldsymbol{\Sigma} \equiv \mathrm{Cov}(\boldsymbol{X})$ exist and the distribution of $\boldsymbol{X}$ is determined by $\boldsymbol{\mu}$ and $\boldsymbol{\Sigma}$. The $m-$variate normal distribution of the random vector $\boldsymbol{X}$ will be denoted by $N_m(\boldsymbol{\mu}, \boldsymbol{\Sigma})$.

Let $\boldsymbol{X}_1 \ \ldots \ \boldsymbol{X}_N$ be a random sample of size N from an $m-$variate distribution $N_m(\boldsymbol{\mu}, \boldsymbol{\Sigma})$. Let

$$\hat{\boldsymbol{X}} = \frac{1}{N}\sum_{i=1}^{N}\boldsymbol{X}_i \tag{B.6}$$

Define

$$\boldsymbol{A} = \sum_{i=1}^{N}(\boldsymbol{X}_i - \hat{\boldsymbol{X}})(\boldsymbol{X}_i - \hat{\boldsymbol{X}})' \tag{B.7}$$

Also,

$$\boldsymbol{S} = \frac{1}{n}\boldsymbol{A} \tag{B.8}$$

where $n = N - 1$. The $m \times m$ matrix $\boldsymbol{S}$ is called the *sample covariance matrix* and it is an unbiased estimate of $\boldsymbol{\Sigma}$, i.e. $E(\boldsymbol{S}) = \boldsymbol{\Sigma}$. To see this write $\boldsymbol{A}$ as

$$\begin{aligned}
\boldsymbol{A} &= \sum_{i=1}^{N}[(\boldsymbol{X}_i - \boldsymbol{\mu})] - (\hat{\boldsymbol{X}} - \boldsymbol{\mu})][(\boldsymbol{X}_i - \boldsymbol{\mu})] - (\hat{\boldsymbol{X}} - \boldsymbol{\mu})]' \\
&= \sum_{i=1}^{N}(\boldsymbol{X}_i - \boldsymbol{\mu})(\boldsymbol{X}_i - \boldsymbol{\mu})' - N(\hat{\boldsymbol{X}} - \boldsymbol{\mu})(\hat{\boldsymbol{X}} - \boldsymbol{\mu})'
\end{aligned}$$

Then,

$$\begin{aligned}
E(\boldsymbol{A}) &= \sum_{i=1}^{N}E[(\boldsymbol{X}_i - \boldsymbol{\mu})E[(\boldsymbol{X}_i - \boldsymbol{\mu})'] - N(\hat{\boldsymbol{X}} - \boldsymbol{\mu})(\hat{\boldsymbol{X}} - \boldsymbol{\mu})'] \\
&= N\boldsymbol{\Sigma} - N\frac{1}{N}\boldsymbol{\Sigma} \\
&= (N-1)\boldsymbol{\Sigma} \\
&= n\boldsymbol{\Sigma}
\end{aligned}$$

so that $E(n^{-1}\boldsymbol{A}) = E(\boldsymbol{S}) = \boldsymbol{\Sigma}$. Now if $l_1 > \ \ldots \ > l_m$ be the eigenvalues of $\boldsymbol{S}$. These are distinct with probability one and are estimates of the eigenvalues $\lambda_1 \geq \ldots \geq \lambda_m$ of $\boldsymbol{\Sigma}$.

References

[1] M. D. Austin and G. L. Stüber. "In-Service Signal Quality Estimation for TDMA Cellular Systems". In *Proc. PIMRC'95*, pp. 836-840, Toronto, Canada, Sep. 1995.

[2] S. Ariyavisitakul "SIR-based power control in a CDMA system". in IEEE Global telecommunications Conference, 1992, pp.868-873.

[3] R. Beck and H. Panzer. "Strategies for Handover and Dynamic Channel Allocation in Micro-Cellular Mobile Radio Cellular Systems". In *Proc. IEEE 39th Vehicular Technology Conference*, pp. 742-748, San Francisco, CA., May 1989.

[4] A. L. Brandão, L. B. Lopez and D. C. McLernon. "Cochannel Interference Estimation for M-ary PSK Modulated Signals" *Wireless Personal Communications*, Vol. 1, No. 1, pp. 23-32, 1994.

[5] A. L. Brandão, L. B. Lopez and D. C. McLernon. "Quality Assessment for Pre-Detection Diversity Switching". In *Proc. PIMRC'95*, pp. 577-581, Toronto, Canada, Sep. 1995.

[6] S. Yoshida, A. Hirai, G. L. Tan, H. Zhou and T. Takeuchi. "In-Service Monitoring of Multipath Delay-Spread and C/I for QPSK Signal". In *Proc. IEEE 42nd Vehicular Technology Conference*, pp. 592-595, Denver, CO., Apr. 1992.

[7] W. Jakes. *Microwave Mobile Communications.* John Wiley and Sons, 1974.

[8] R. D. Yates. "A Framework for Uplink Power Control in Cellular Radio Systems". *IEEE JSAC*, Vol. 13, No. 7, Sep. 1995.

[9] M. Andersin, N.B. Mandayam, and R. Yates, "Subspace based SIR Estimation for TDMA Cellular Systems," To Appear in *"Special Issue on Power Control" IEEE/ACM Transactions on Networking*, 1996

[10] E. A. Frech and C. L. Mesquida. "Cellular Models and Hand-off Criteria," *IEEE Vehicular Technology Conference"*, pp. 128-35, 1989.

[11] EIA/TIA Interim Standard-95, 'Mobile Station — Base Station Compatibility Standard for Dual-Mode Wideband Spread Spectrum Cellular Systems,' July 1993.

[12] S. Kozono. "Co-channel Interference Measurement Method for Mobile Communication". *IEEE Trans. on Vehicular Technology*, Vol. 36, pp. 7-13, 1987.

[13] J. Z. Wang. Simulation and performance analysis of dynamic channel allocation algorithms in DECT". *IEEE Trans. on on Vehicular Technology*, Vol. 42, No. 4, pp. 563-569, 1993.

[14] J. Zander. "Performance of Optimum Transmitter Power Control in Cellular Radio Systems". *IEEE Trans. on Vehicular Technology*, Vol. 41, No. 1, Feb. 1992.

[15] G. Bienvenu and L. Kopp. "Optimality of high resolution array processing using the eigensystem approach". *IEEE Trans. on ASSP*, Vol.31, pp.1235-1248, 1983.

[16] R. Muirhead. *Aspects of Multivariate Statistical Theory.* New York: John Wiley and Sons, 1982.

[17] J. Proakis. *Digital Communications.* McGraw-Hill, second ed., 1989.

[18] M. Wax and T. Kailath. "Detection of Signals by Information Theoretic Criteria". *IEEE Trans. on ASSP*, ASSP-33(2), pp. 387-392, Apr. 1985.

[19] T. Cover and J. Thomas *Elements of Information Theory.* John Wiley and Sons, second ed., 1991.

[20] S. Haykin, J. Litva and T. J. Shepherd. *Radar Array Processing*, Springer Series in Information Sciences, Vol.25, Springer-Verlag Berlin, Heidelberg 1993.

[21] D. N. Lawley "Tests of significance for the latent roots of covariance and correlation matrices."*Biometrika*, 43, pp.128-136, 1956.

[22] K. Kim. "On the Error Probablity of a DS/SSMA System with a Non-coherent M-ary Orthogonal Modulation". In *Proc. IEEE 42nd Vehicular Technology Conference*, pp. 482-485, Denver, CO., May 1992.

[23] L. C. Zhao, P. R. Krishnaiah and Z. D. Bai. "On Detection of the Number of Signals in Presence of White Noise". *Journal of Multivariate Analysis*, 20:1:1-25, 1986.

[24] B. Yang. "Projection Approximation Subspace Tracking". *IEEE Trans. on Signal Processing*, Vol.43, pp. 95-107, Jan. 1995.

[25] P. Comon and G. H. Golub. "Tracking a few extreme singular values and vectors in signal procesing". *Proc. of IEEE*, pp. 1327-1343, Aug. 1990.

[26] N. L. Owsley. "Adaptive data orthogonalization" *Proc. IEEE ICASSP*, pp. 109-112, 1078.

[27] K. C. Sharman. "Adaptive algorithms for estimating the complete covariance eigenstructure" in *Proc. IEEE ICASSP* , pp.1401-1404, Tokyo, Japan, Apr. 1986

[28] M. Moonen, P. Van Dooren and J. Vandewalle. "Updating singular value decompositions: A parallel implementation ." in *Proc. SPIE Adv. Algorithms Architectures Signal Processing*, pp. 80-91, Aug. 1989, San Diego, CA.

[29] R. Bunch, C. P. Nielsen and D. Sorenson. "Rank-one modification of the symmetric eigenproblem." *Numerische Mathematik*, vol 31, pp. 31-48, 1978.

[30] X. Wang and H. V. Poor. "Blind Adaptive Interference Suppression for CDMA Communications Bades on Eigenspace Tracking." *Proceedings of CISS*, Baltimore, MD, March 1997.

[31] G. W. Stewart. "An updating algorithm for subspace tracking". *IEEE Trans. on Signal Processing*, vol. 40, pp. 1535-1541, 1992.

[32] C. H. Bischof and G. M. Shroff. "On updating signal subspaces." *IEEE Trans. on Signal Processing*, vol. 40, pp. 96-105, 1992.

[33] J. Yang and M. Kaveh. "Adaptive eigenspace algorithms for direction or frequency estimation and tracking". *Proc. IEEE Trans. Acoust.,Speech.,Signal Processing*, vol. 36, pp. 241-251, 1988.

[34] S. Bannour and M. R. Azimi-Sadjadi. "An adaptive approach for optimal data reduction using recursive least squares learning method." *Proc. IEEE ICASSP*, pp. 11297-11300, Mar. 1992, San Francisco, CA.

[35] G. Strang. *Linear algebra and its applications.* Harcourt Brace Jovanovich College Publishers, 1988.

[36] M. Gudmundson. "Correlation Model for Shadow Fading in Mobile Radio Systems." *Electronic Letters*, Vol. 27, No. 23, pp. 2145-2146. Nov. 1991.

[37] A. Papoulis. Probability, Random Variables, and Stochastic Processes. McGraw-Hill Publishers, 1984.